資料１
レジストリ解析結果

本研究の概要

- 本邦における患者像の把握
- 病型分類に基づいた診療実態の把握
- 経過（特に重症例）の把握

診断・治療法の標準化
重症度判定のValidation

質の高い診療の均霑化
ガイドライン作成

他の難治性疾患では
数多くレジストリ調査が
行われている

2017～ICでも開始

登録施設の増加

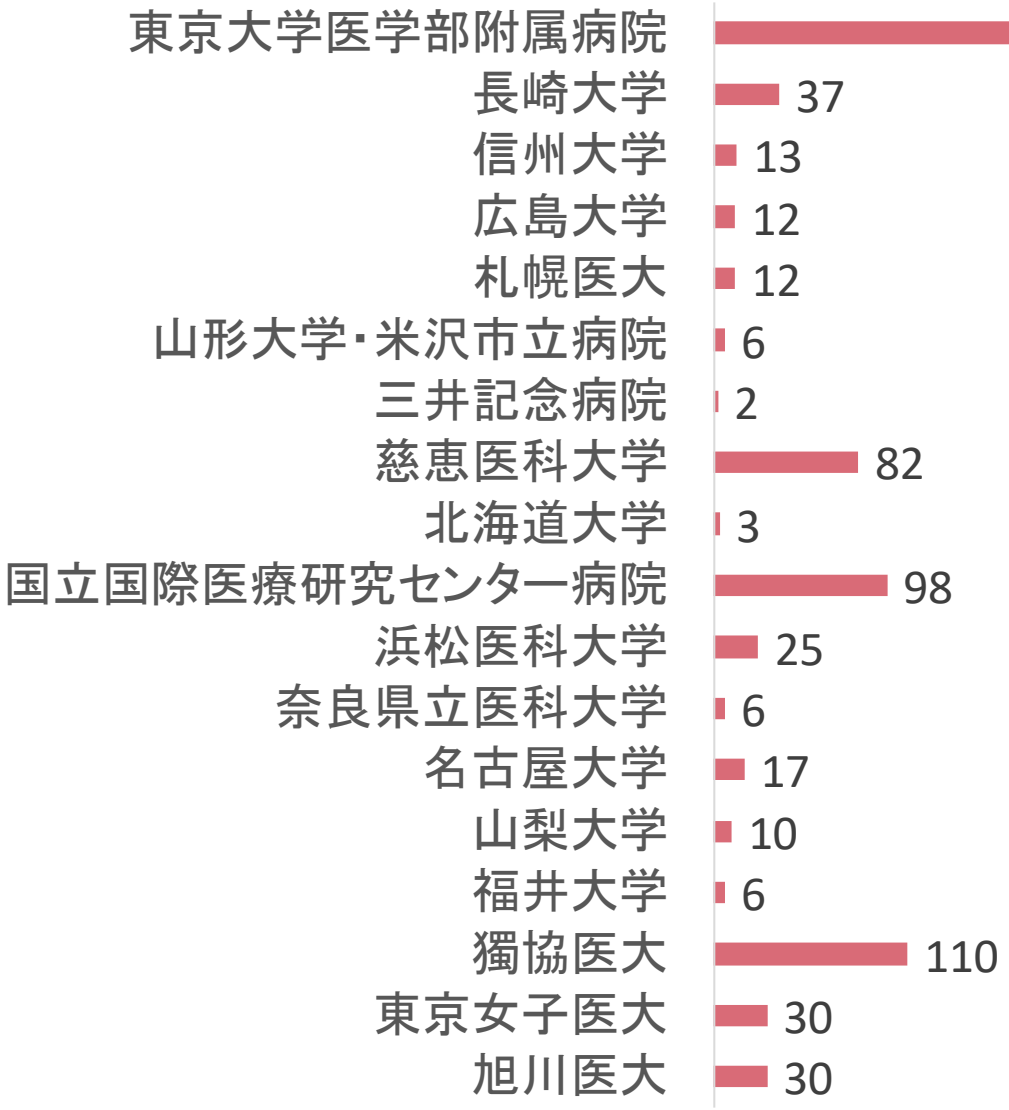
東京大学医学部附属病院 363
長崎大学 37
信州大学 13
広島大学 12
札幌医大 12
山形大学・米沢市立病院 6
三井記念病院 2
慈恵医科大学 82
北海道大学 3
国立国際医療研究センター病院 98
浜松医科大学 25
奈良県立医科大学 6
名古屋大学 17
山梨大学 10
福井大学 6
獨協医大 110
東京女子医大 30
旭川医大 30

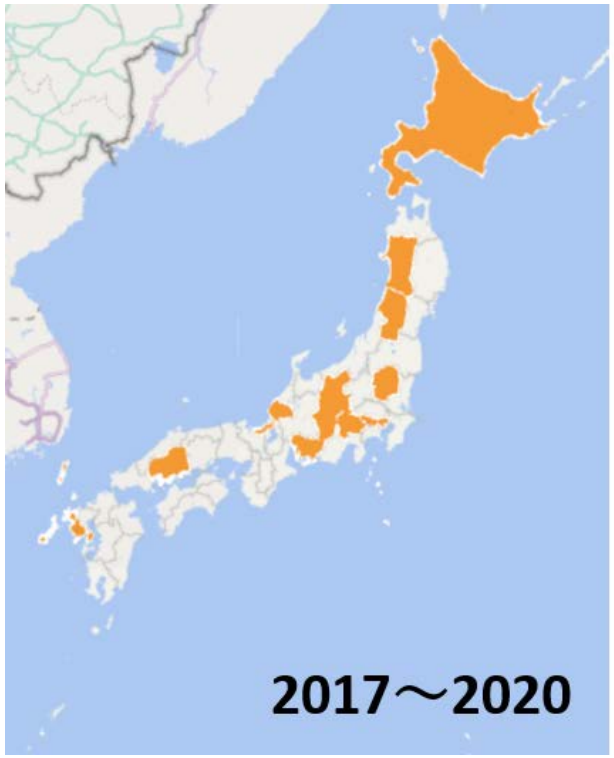
2017～2020

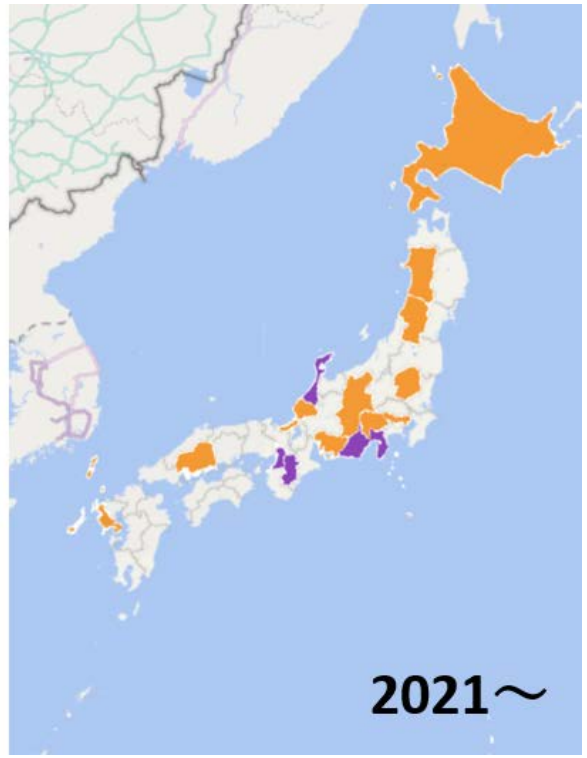
2021～

病型分類

- 対象データ：2023年11月9日時点までに入力されたデータ
- 登録人数：間質性膀胱炎レジストリに登録された909名
- 分析対象: 症例タイプ設問に回答のある862名
- ※欠損値を除外して集計したため、合計は862にならないことがある

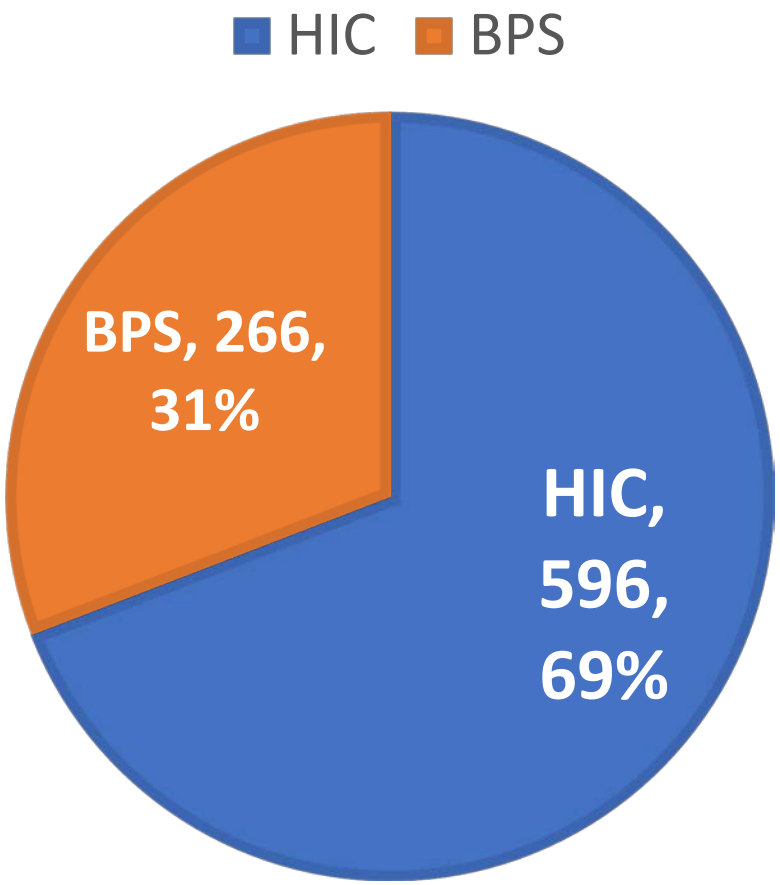

性差

全体

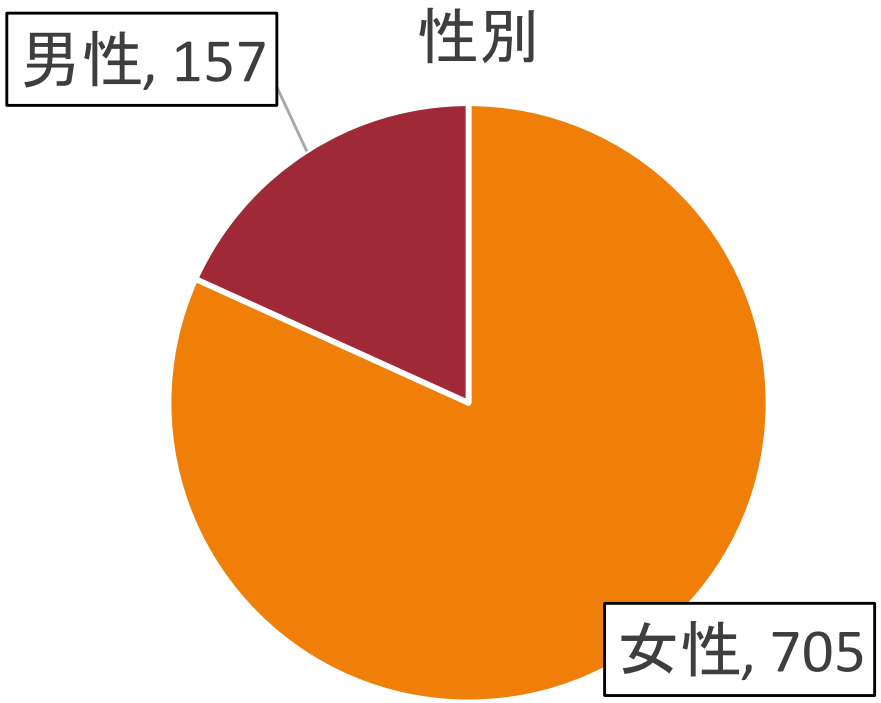

BPS

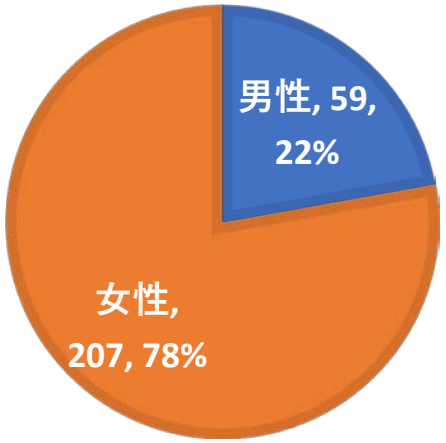

HIC

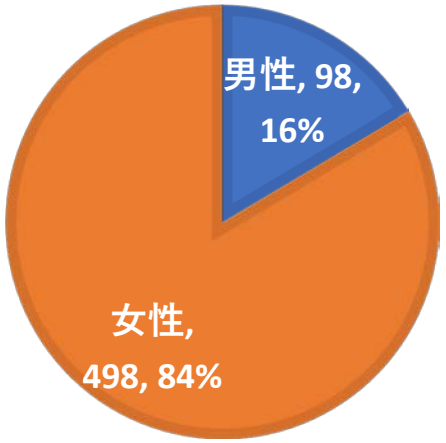

参考）国外では？

Author	Year	Sample Number	Cystoscopy performed	Gender Male(%)	Hunner type (%)
Holm-Bentzen M.	1987	115	115	-	3.5
Simon L.J.	1997	424	190	8.5	10.5
Hanno P.M. (NIDDK)	1999	379	101	Female only	-
Peeker R.	2002	231	231	-	55
Peters K. M.	2007	87	87	Female only	-
Richter B.	2010	349	349	7.5	8.0
Logadottir Y	2012	379	379	16	57.2
Griffith J.W.	2016	424	No	45.0	-
Yu W.R.	2020	486	486	13.4	3.91

HICとBPSを混ぜて解析した結果か…

年代

全体

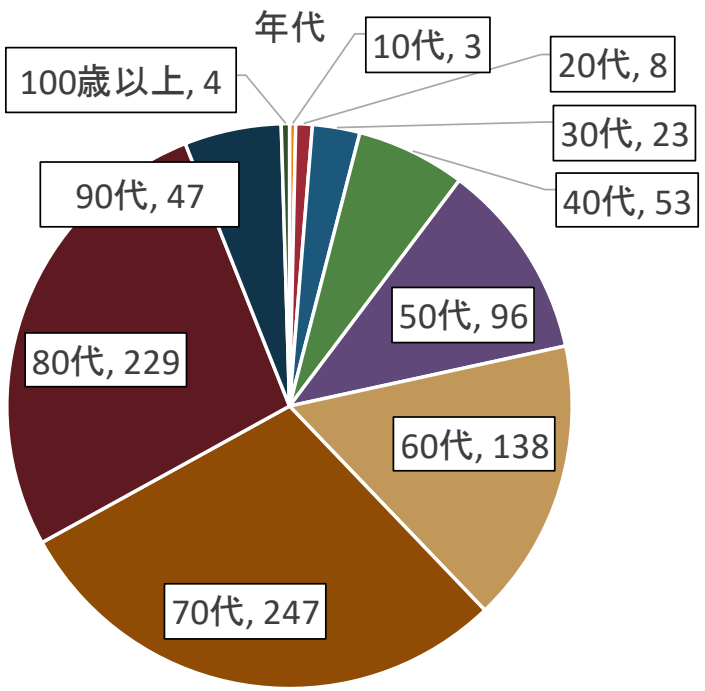

BPS（N=266）

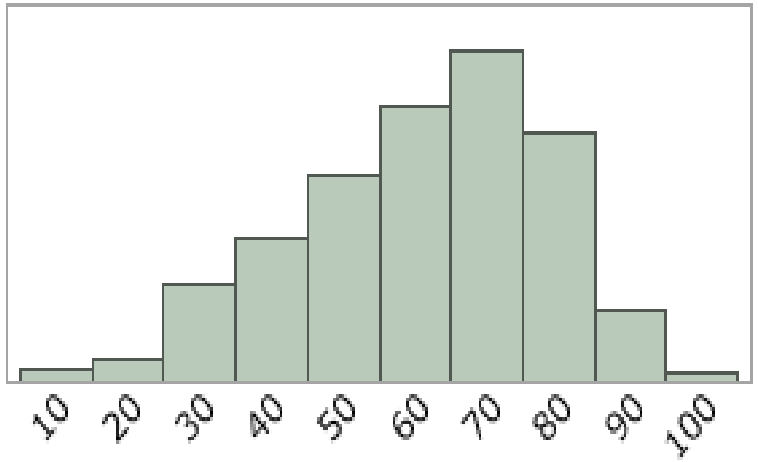

HIC（N=584）

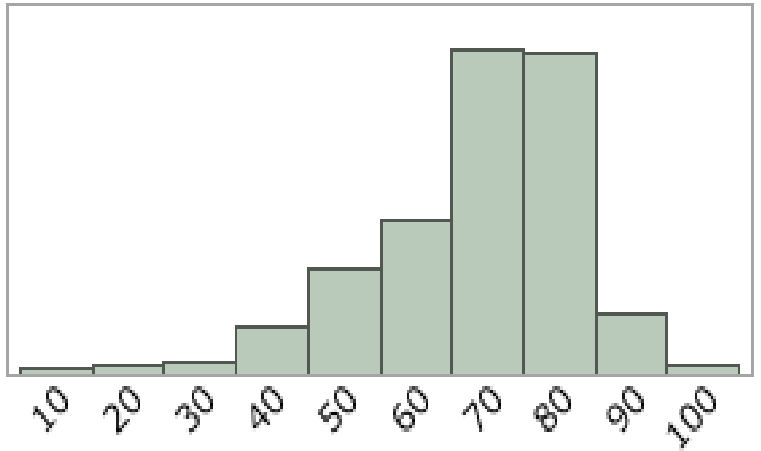

参考）令和3年受給者数（N=885）

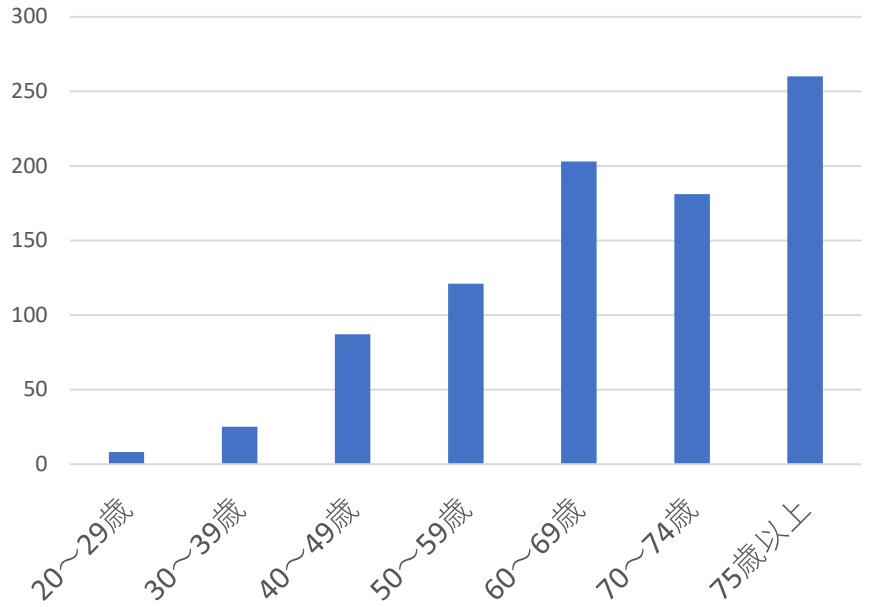

既往歴

	全体(n=862)		男性(n=157)		女性(n=705)	
	n	%	n	%	n	%
過活動膀胱	94	10.9%	8	5.1%	86	12.2%
腹圧性尿失禁	5	0.6%	0	0.0%	5	0.7%
尿路結石	11	1.3%	5	3.2%	6	0.9%
尿路感染症	78	9.0%	11	7.0%	67	9.5%
骨盤臓器脱	25	2.9%	0	0.0%	25	3.5%
尿道狭窄	21	2.4%	9	5.7%	12	1.7%
膀胱頸部硬化症	1	0.1%	1	0.6%	0	0.0%
前立腺肥大症	27	3.1%	27	17.2%	0	0.0%
線維筋痛症	5	0.6%	1	0.6%	4	0.6%
自己免疫性疾患	83	9.6%	8	5.1%	75	10.6%
炎症性腸疾患	3	0.3%	0	0.0%	3	0.4%
過敏性腸症候群	13	1.5%	3	1.9%	10	1.4%
脊椎疾患	65	7.5%	17	10.8%	48	6.8%
神経疾患	49	5.7%	11	7.0%	38	5.4%
うつ病	52	6.0%	6	3.8%	46	6.5%
アレルギー	83	9.6%	12	7.6%	71	10.1%
癌	92	10.7%	19	12.1%	73	10.4%
該当なし	321	37.2%	59	37.6%	262	37.2%

既往歴

	HIC (n= 352)	BPS (n=177)	P value
OAB	75	19	0.02
SUI	3	2	0.65
Urolithiasis	6	5	0.33
UTI	67	11	0.0005
POP	14	11	0.17
Urethral stricture	10	11	0.05
BPH	18	9	0.83
Fibromyalgia	2	3	0.17
Autoimmune disease	68	15	0.008
SjS	33	10	0.32
RA	19	1	0.001
SLE	5	0	0.33
IBD	3	0	0.56
IBS	6	7	0.13
LSCS	37	28	0.03
Neurodegenerative disease	36	13	0.03
Depression	28	24	0.02
Allergy	54	29	0.38
Cancer	72	20	0.06

Fisher's test

手術歴

全体

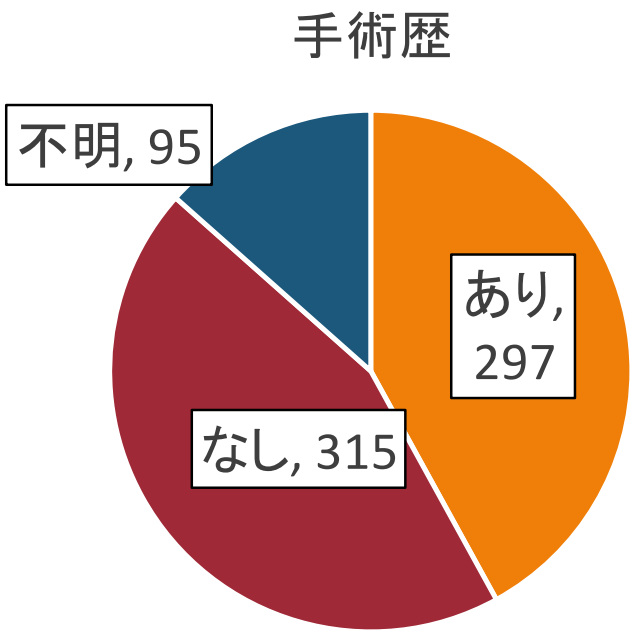

手術内容の内訳

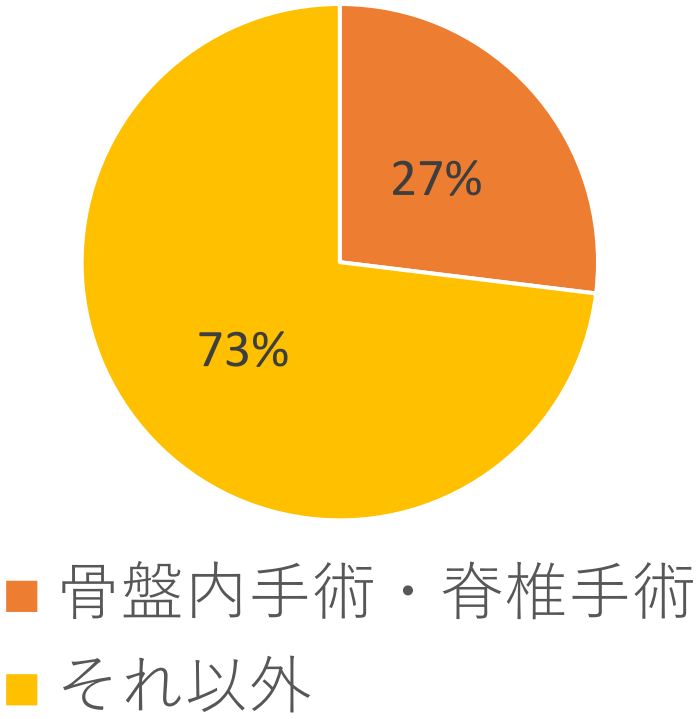

家族歴

全体

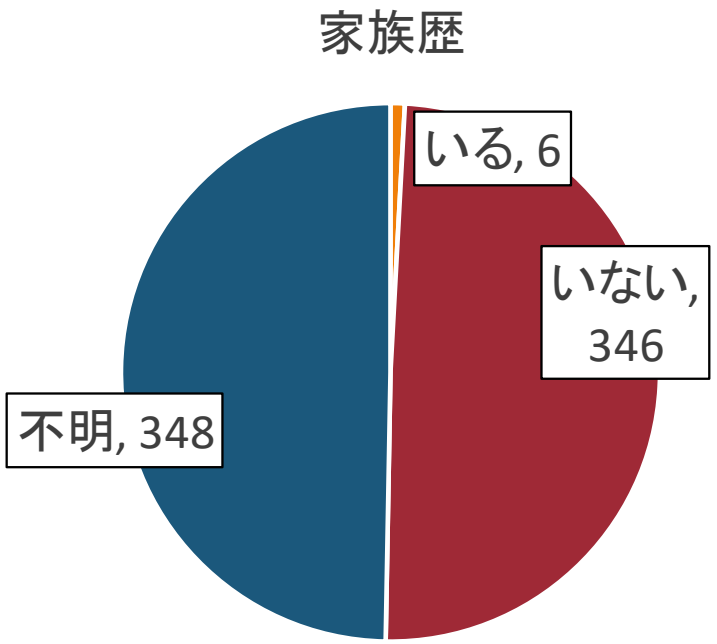

家族歴アリ　6名の内訳

HIC	BPS
母	双子の姉
夫（除外すべき）	双子の妹
	妹
	母

食事との関係

全体

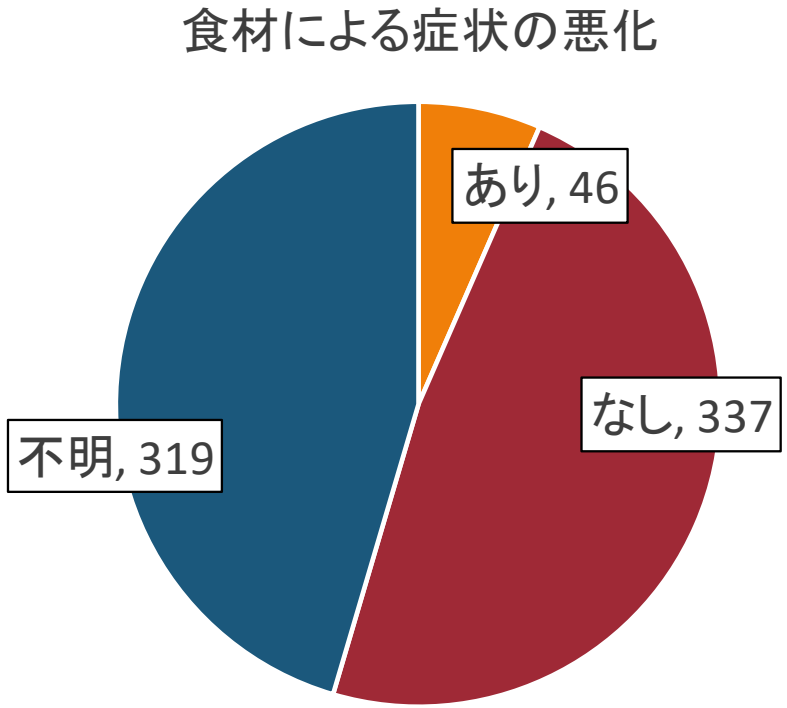

	HIC	BPS
食事関係あり	36	10
なし	163	174
不明	237	82

症状悪化する食品の内訳

	全体	HIC	BPS
アルコール	8	4	4
カフェイン含有飲料（合計）	12	6	6
カフェイン	2	2	0
コーヒー	8	4	4
緑茶	1	0	1
コーラ	1	0	1
果物（合計）	13	10	3
特記なし	2	1	1
柑橘類	10	8	2
ぶどう	1	1	0
香辛料（合計）	19	12	7
香辛料・刺激物（特記なし）	10	6	4
香辛料（唐辛子・和辛子）	2	2	0
香辛料（生姜）	2	1	1
香辛料（にんにく）	1	0	1
カレー	4	3	1
大豆製品（合計）	8	6	2
特記なし	2	2	0
味噌汁、納豆	1、1	1,1	0
豆腐	2	2	1
醤油	1	0	1

症状悪化する食品の内訳

	全体	HIC	BPS
乳製品（合計）	4	1	3
牛乳、生クリーム、チーズ	2、1、1	1	3
チョコレート	1	0	1
野菜（合計）	3		
生野菜	1		
ほうれん草、トマト、しそ	1、1，1		
そば	1	1	0
すし	1	0	1
酢の物	2	2	0
みりん	1		1
塩分がつよいもの	2	0	2
生卵	2		1
肉	2	0	2
魚（内刺身１）	3	1（刺身）	2

相互関係の乏しい５種類以上の食品に対して悪化と答えた症例が３例
いずれもBPS

症例１
鮨、生姜、にんにく、醤油、みりん、緑茶

症例２
塩分強いもの、肉、魚、コーラ、コーヒー、アルコール、乳製品

症例３
塩分全般、肉、牛乳、生卵、チョコレート、コーヒ、アルコール

罹患期間・診断前期間

罹患期間

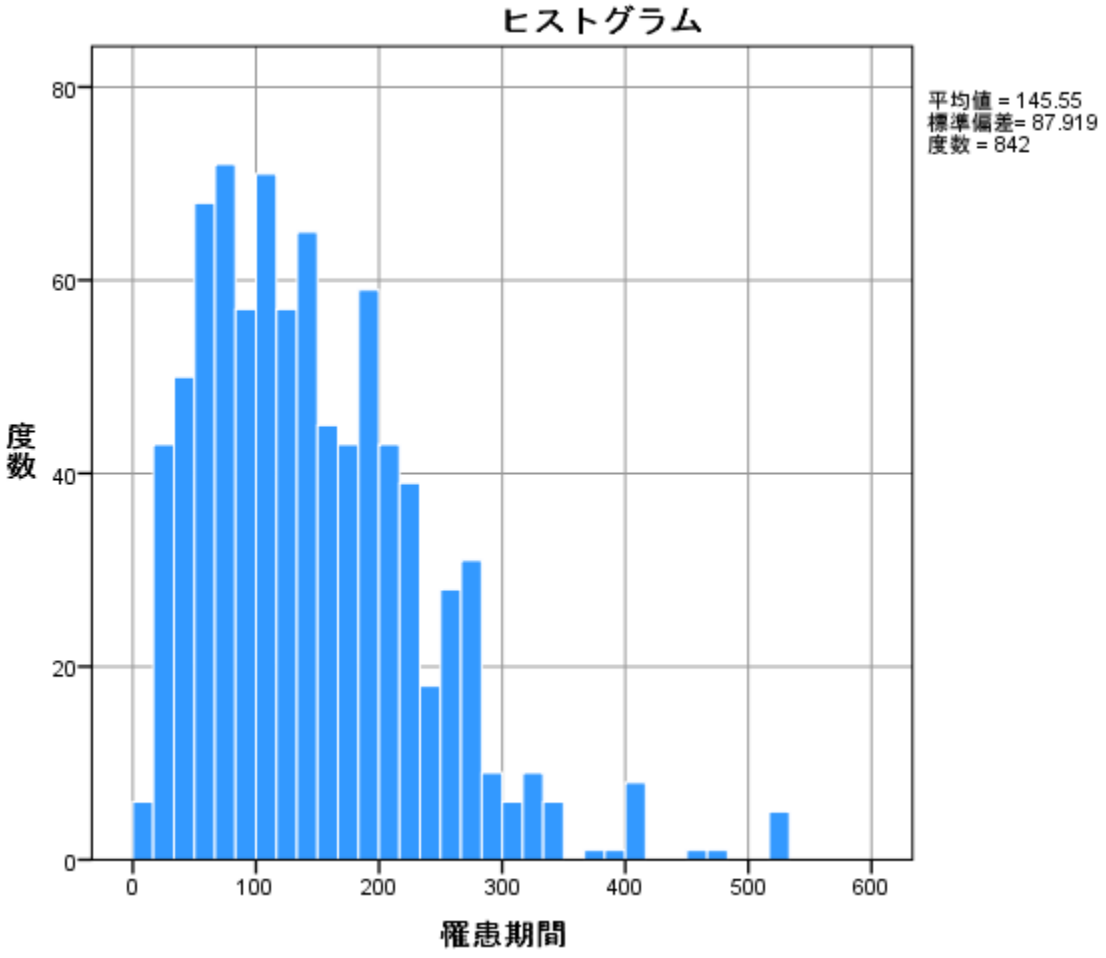

診断前期間

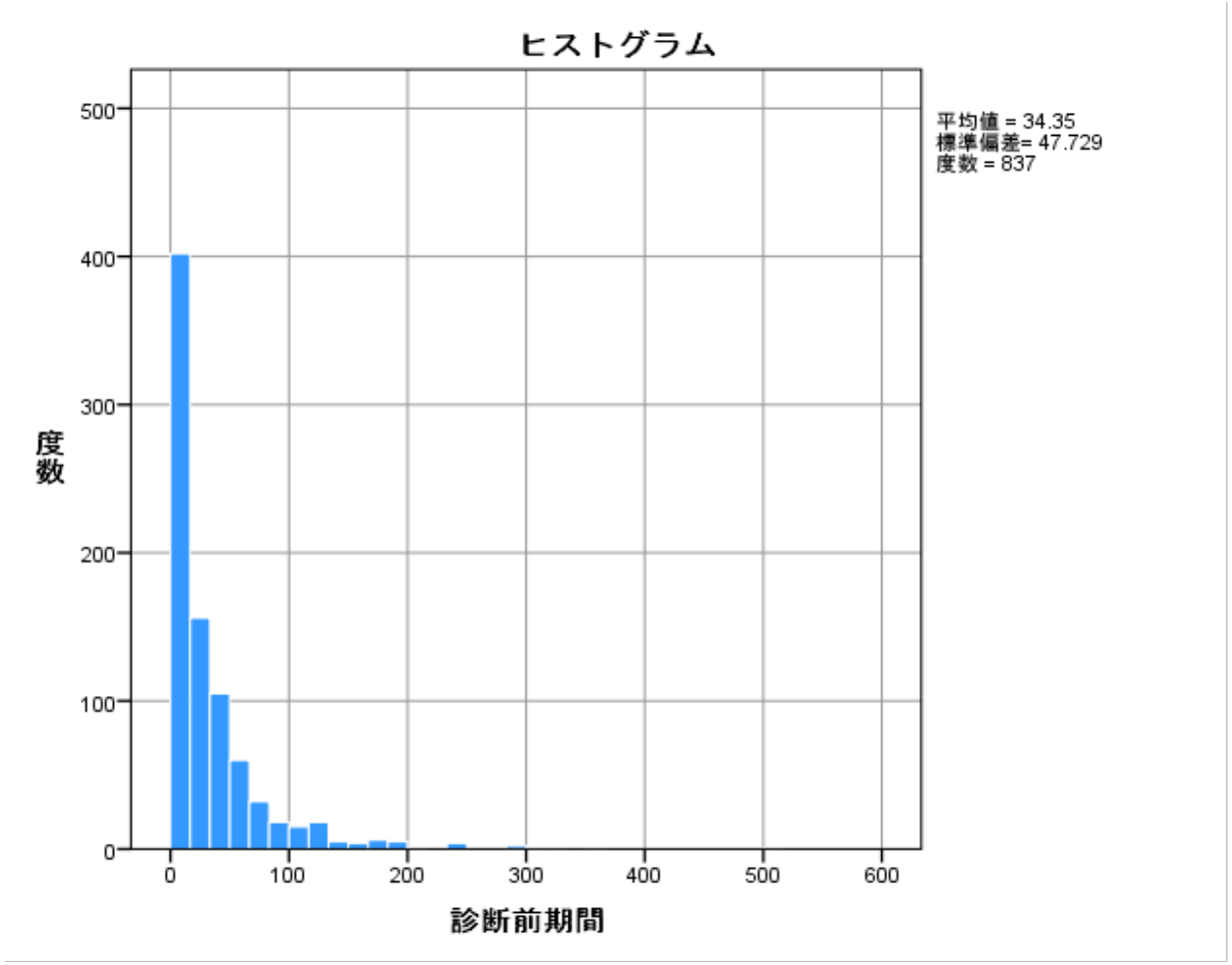

受診病院数

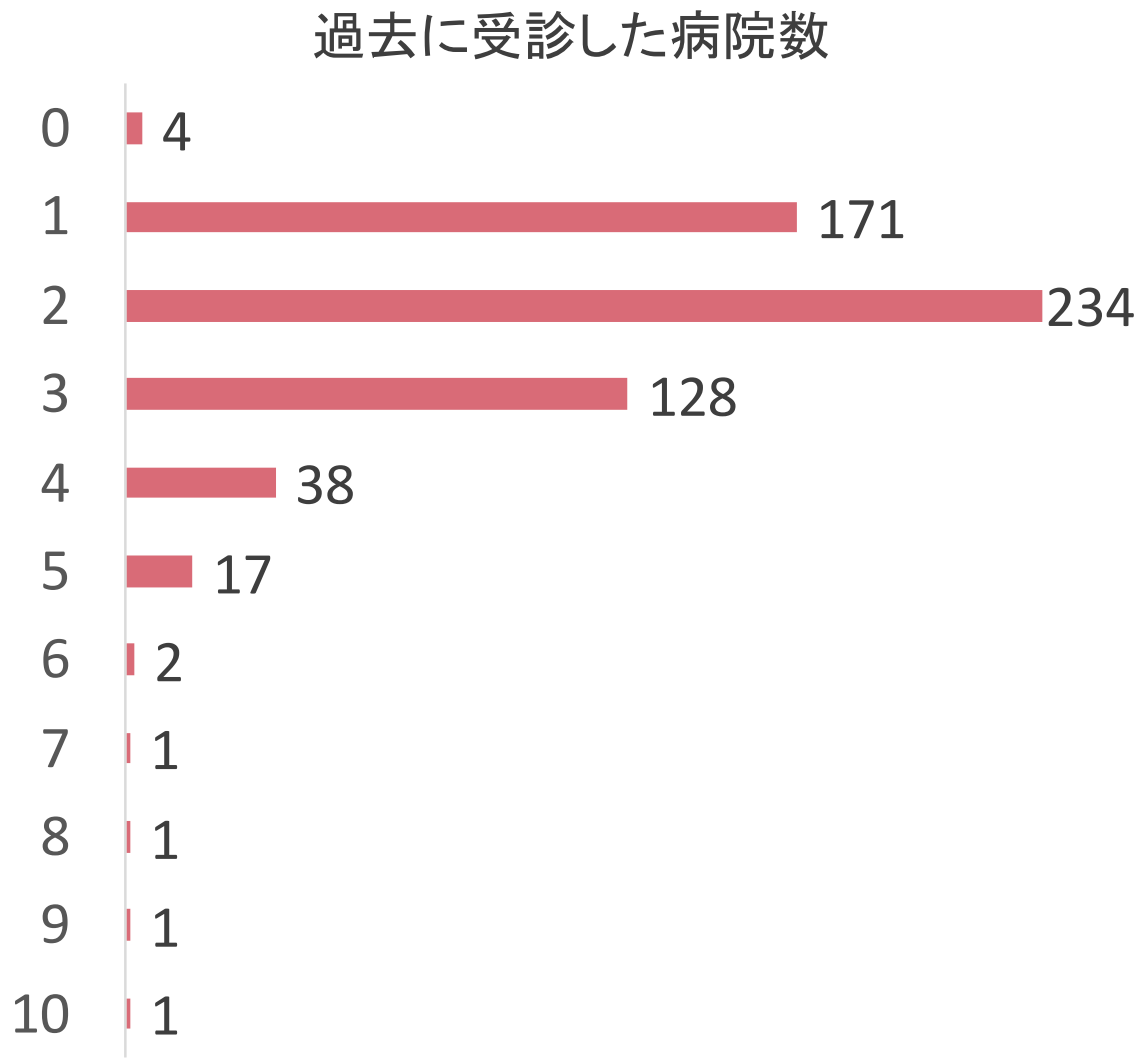

OSSI

全体

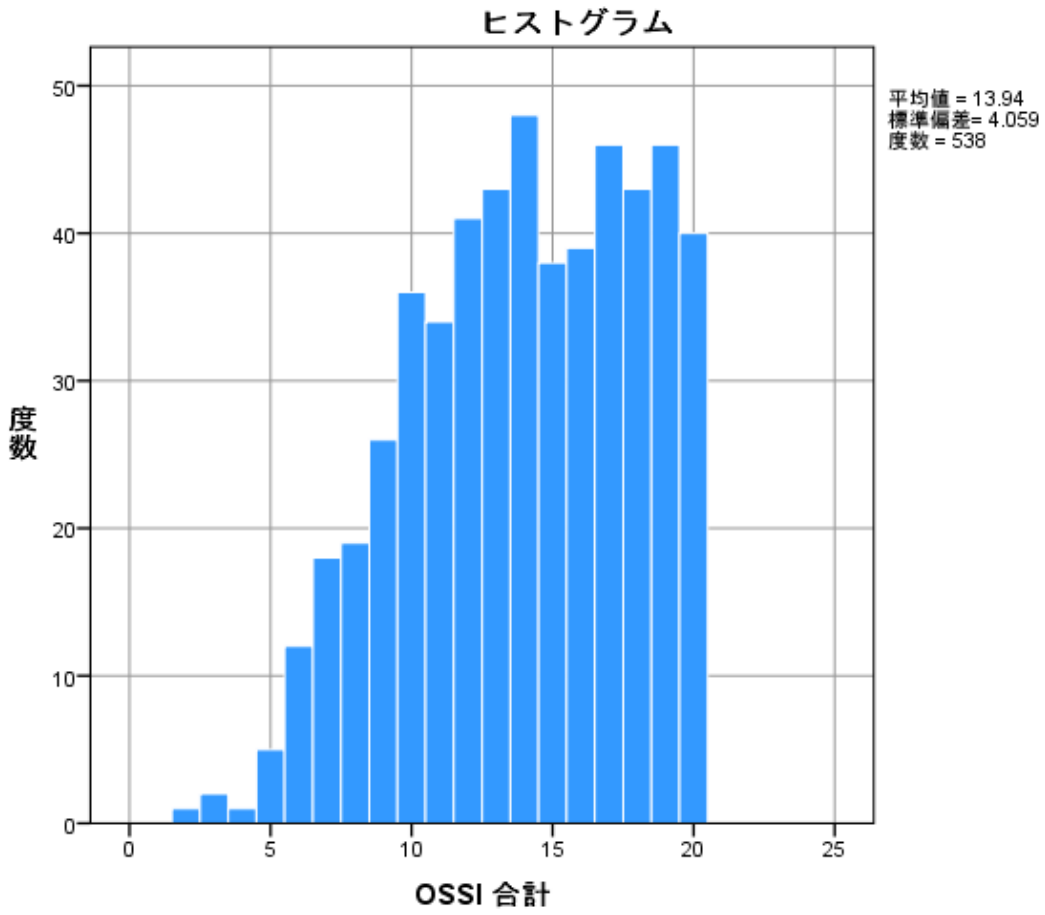

BPS

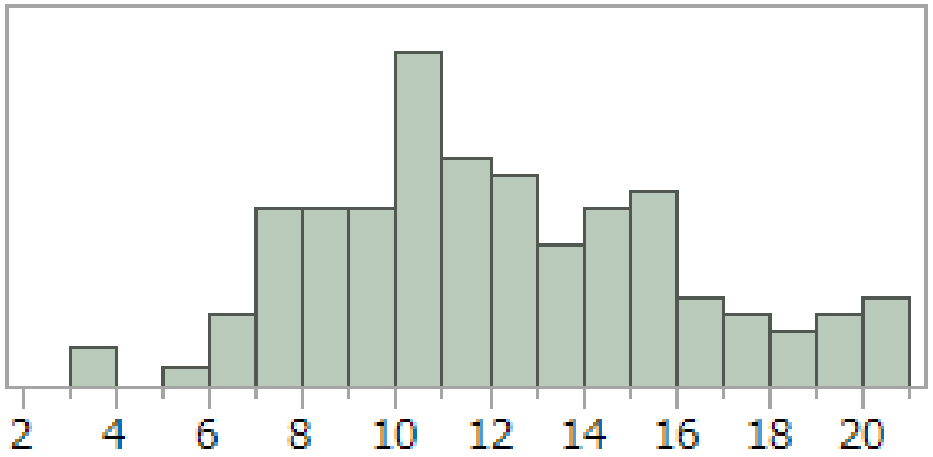

HIC

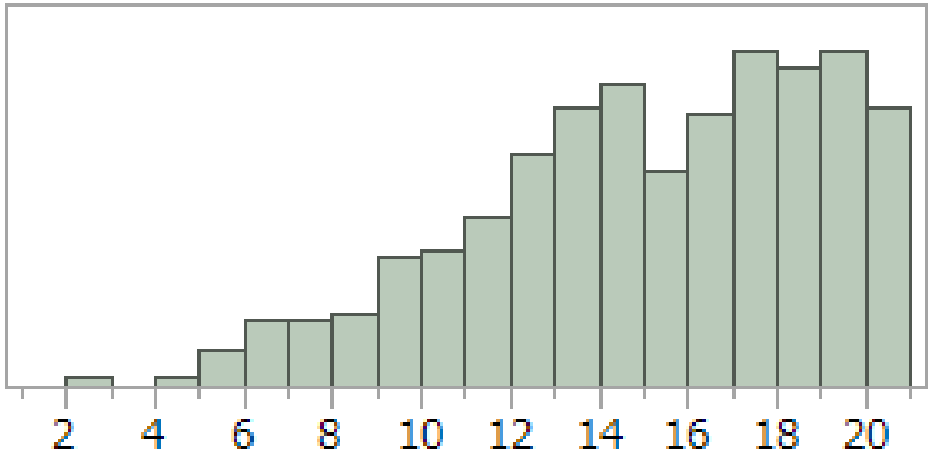

OSSI

	HIC(n=407)	BPS(n=131)	P value
OSSI Q1 (urge)	3.06 ± 1.72	2.59 ± 1.70	0.0066
OSSI Q2 (Daytime frequency)	4.07 ± 1.31	3.61 ± 1.38	0.0006
OSSI Q3 (Nighttime frequency)	3.91 ± 1.21	2.53 ± 1.42	＜0.0001
OSSI Q4 (Pain)	3.06 ± 1.26	3.01 ± 1.556	＜0.0001
OSSI total	14.65 ± 3.88	11.75 ± 3.81	＜0.0001

OSPI・QOL Score・NRS

	HIC(n=407)	BPS(n=131)	p value
OSPI Q1 (Daytime frequency)	3.12 ± 1.06	2.74 ± 1.32	0.0007
OSPI Q2 (Nocturia)	3.29 ± 0.94	2.50 ± 1.38	<0.0001
OSPI Q3 (urge)	2.86 ± 1.20	2.41 ± 1.35	0.0003
OSPI Q4 (pain)	3.30 ± 1.10	2.82 ± 1.28	<0.0001
OSPI total score	12.58 ± 3.34	10.47 ± 3.66	<0.0001
QOL score	5.55 ± 0.84	5.22 ± 1.01	<0.0001
Pain Scale (NRS)	7.44 ± 2.28	6.33 ± 2.50	<0.0001

OABとの類似性　（IC/BPSにおける切迫感）

	HIC(n=352)	BPS(n=176)	p value
OSSI Q1 (urge)	3.06±1.72	2.59±1.70	0.0066
OSSI Q2 (Dytime frequency)	4.07±1.31	3.61±1.38	0.0006
OSSI Q3 (Nighttime frequency)	3.91±1.21	2.53±1.42	＜0.0001
OSSI Q4 (Pain)	3.06±1.26	3.01±1.556	＜0.0001
OSSI total score	14.65±3.88	11.75±3.81	＜0.0001
OSPI Q1 (Daytime frequency)	3.2±1.1	2.8±1.2	0.05
OSPI Q2 (Nocturia)	3.3±1.0	2.6±1.4	<0.0001
OSPI Q3 (urge)	3.0±1.2	2.5±1.4	0.0088
OSPI Q4 (pain)	3.2±1.2	3.0±1.2	0.15
OSPI total score	12.6±3.5	10.9±3.7	0.001
QOL score	5.6±0.9	5.1±1.4	0.0046
Pain Scale (NRS)	7.3±2.3	6.5±2.2	0.0007

症状	点数	頻度
急に我慢できなくなって尿をすることが，どれくらいの割合でありましたか？	0	全くない
	1	5回に1回の割合より少ない
	2	2回に1回の割合より少ない
	3	2回に1回の割合くらい
	4	2回に1回の割合より多い
	5	ほとんどいつも

急に尿を我慢できなくなること	0	困っていない
	1	ほんの少し困っている
	2	少し困っている
	3	困っている
	4	ひどく困っている

IC/BPSの相当数でOAB症状あり

OABSSの質問3で、4～5点相当

3	急に尿がしたくなり、我慢が難しいことがありましたか	0	なし
		1	週に1回より少ない
		2	週に1回以上
		3	1日1回くらい
		4	1日2～4回
		5	1日5回以上

排尿日誌

	HIC(n=502)	BPS(n=211)	p value
24-hour frequency	18.5±8.4	14.4±7.3	＜0.0001
Night time frequency	4.7±2.8	2.7±2.4	＜0.0001
Daytime frequency	13.5±6.6	11.0±5.4	0.0003
Average voided volume (ml)	99.0±51.1	125.9±73.9	＜0.0001
Maximum voided volume (ml)	161.9±80.5	232.9±131.5	＜0.0001
24-hour urine volume (ml)	1572.3±660.0	1510±646.4	0.404
Nocturnal urine volume (ml)	473.1±267.4	358.2±245.3	0.0018
Daytime urine volume (ml)	1068±473.4	1047±480.6	0.745

HICでVV減少、排尿回数増加、夜間尿量多

昼間排尿量・24時間排尿量は有意差なし

水圧拡張術/ハンナ病変焼灼術所見（初回）

		HIC(n=352)	BPS(n=177)	p value
Bladder capacity under anesthesia (ml)		460.0±179.7	661.2±219.3	＜0.0001
Numbers of Hunner lesion				
% of Hunner lesion occupying bladder wall		19.2		
Location of Hunner lesion (n)				
	Neck	4	N/A	
	Trigone	12	N/A	
	Retrotrigone	33	N/A	
	Posterior wall	393	N/A	
	Dome	203	N/A	
	Anterior wall	65	N/A	
	Right lateral wall	261	N/A	
	Left lateral wall	247	N/A	
	Whole bladder	26	N/A	

ハンナ病変の数と占拠率

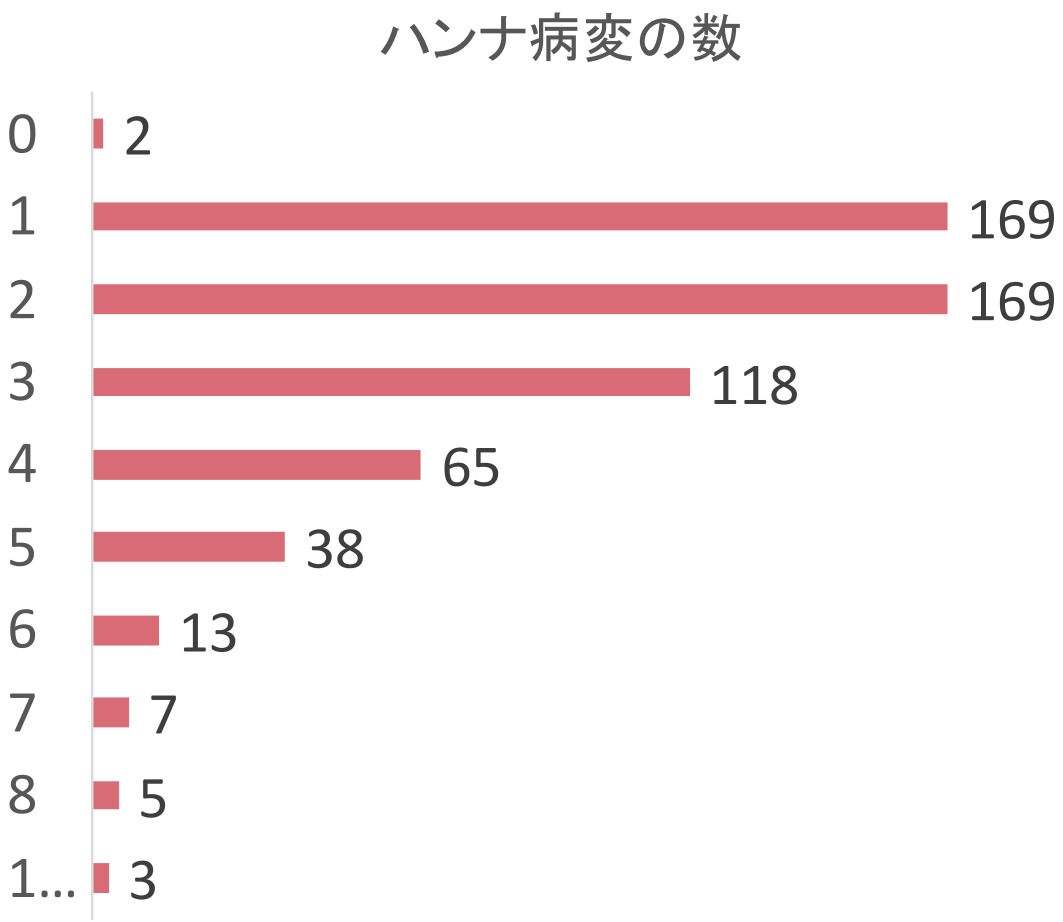

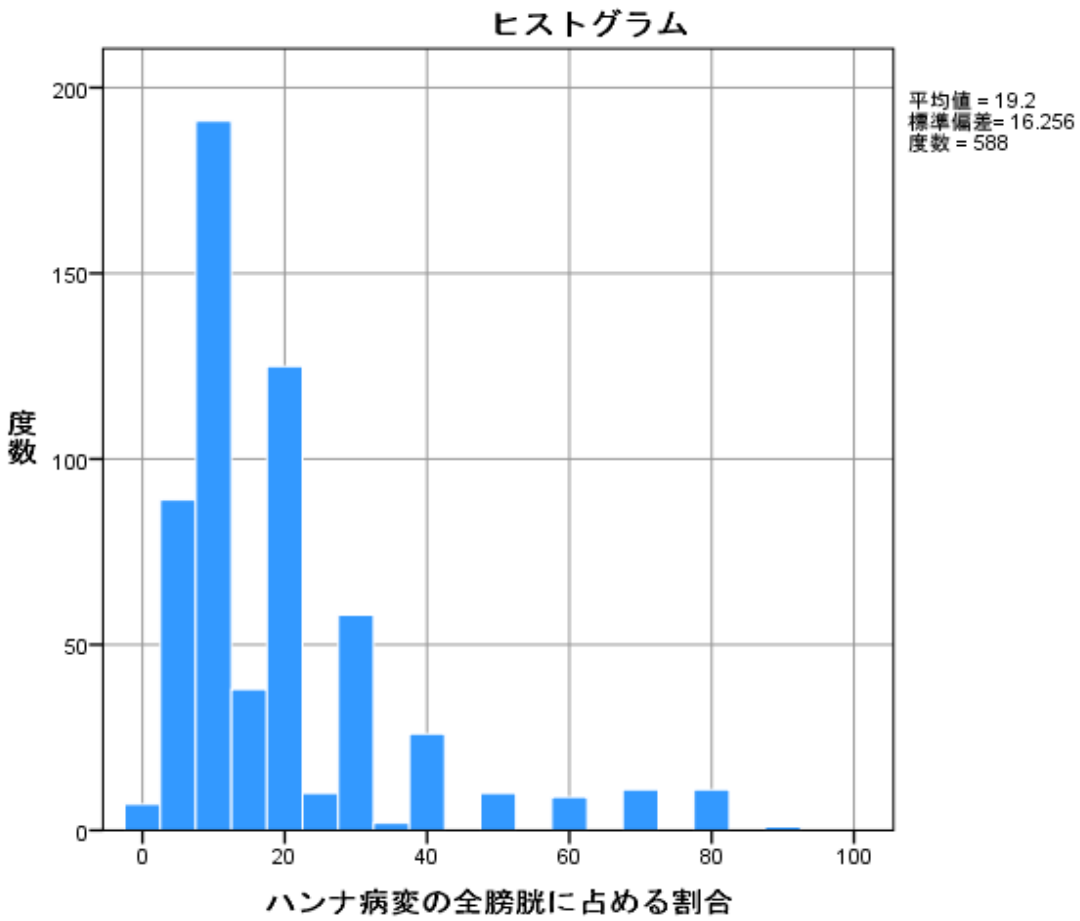

重症度基準

重症度	基　準
重症	膀胱痛の程度＊が７点から10点　かつ 排尿記録による最大一回排尿量が100mL以下
中等症	重症と軽症以外
軽症	膀胱痛の程度＊が０点から３点　かつ 排尿記録による最大一回排尿量が200mL以上

＊膀胱痛の程度（０～10点）の質問

膀胱の痛みについて、「全くない」を０、想像できる最大の強さを10としたとき、平均した強さに最もよくあてはまるものを１つだけ選んで、その数字に○を付けてください
0　1　2　3　4　5　6　7　8　9　10

診断基準の問題点

【問題点】

現行の重症度基準は、IC研究会で設定されたempiricalな値

国外では同類の重症度基準は存在しない

【現在行われていること】

① 重症度基準のValidtion

② 基準を緩やかにするべきか？→難病指定患者　増

厳しくすべきか？　→難病指定患者　減

現状維持

③ 重症例の長期予後　重症化する症例を早期に見極められるか？

レジストリ登録症例での重症度分布

HIC

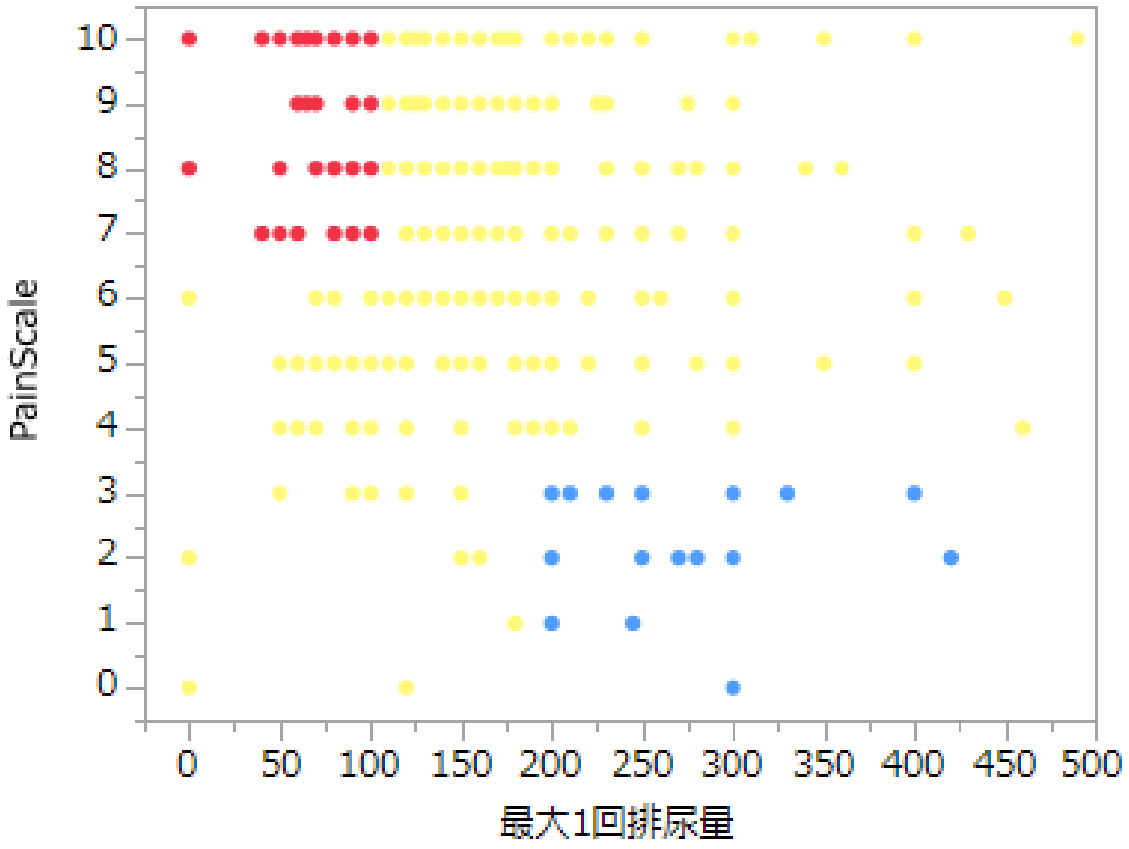

軽症4％　中等症76％　重症20％

BPS

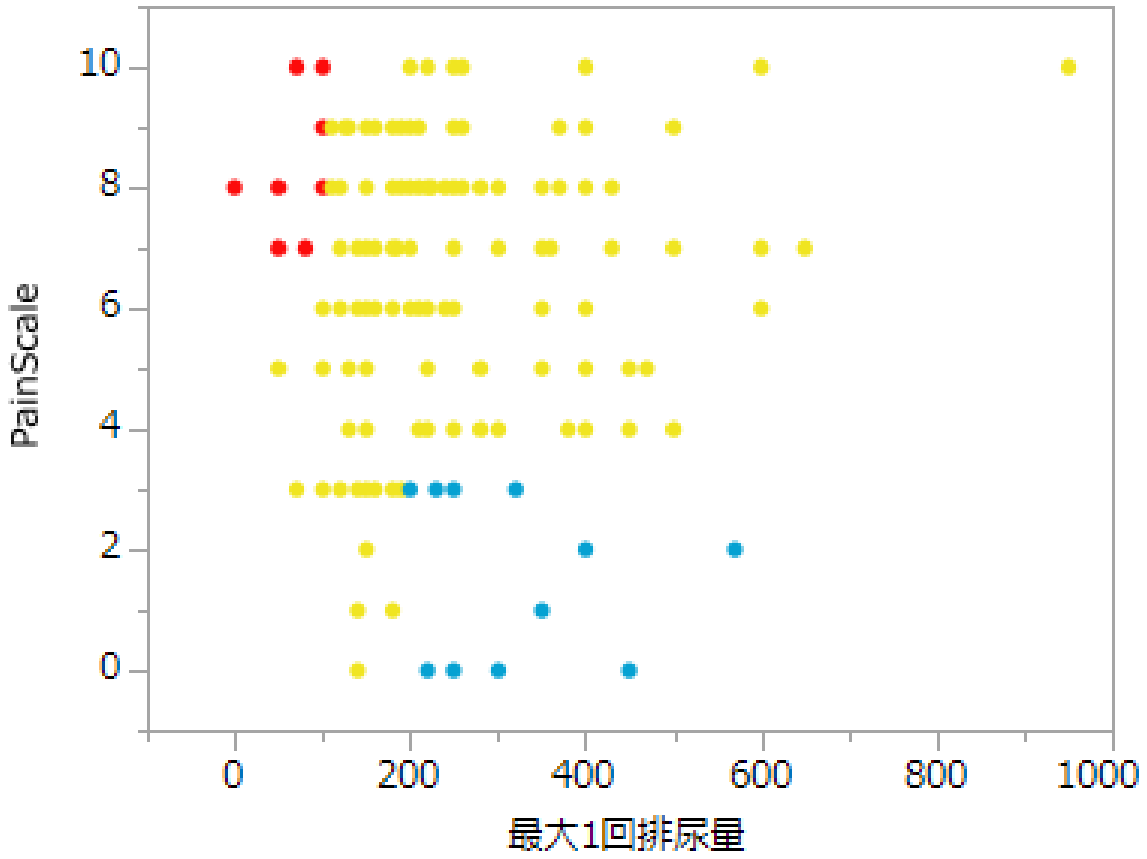

軽症6％　中等症89％　重症5％

現行の重症度基準では　約80％の症例が中等症

重症度分類とOSSI

HIC

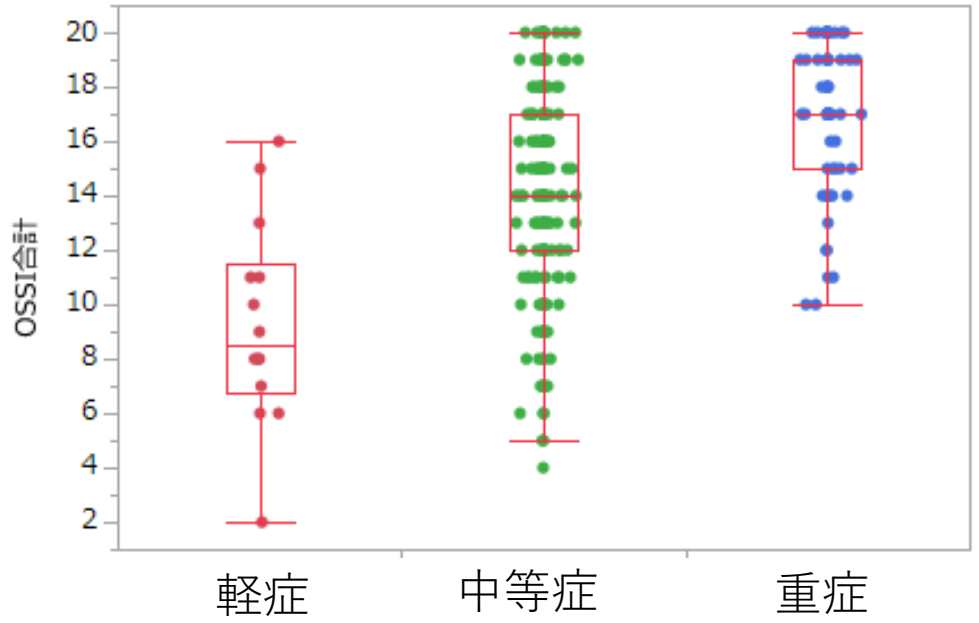

BPS

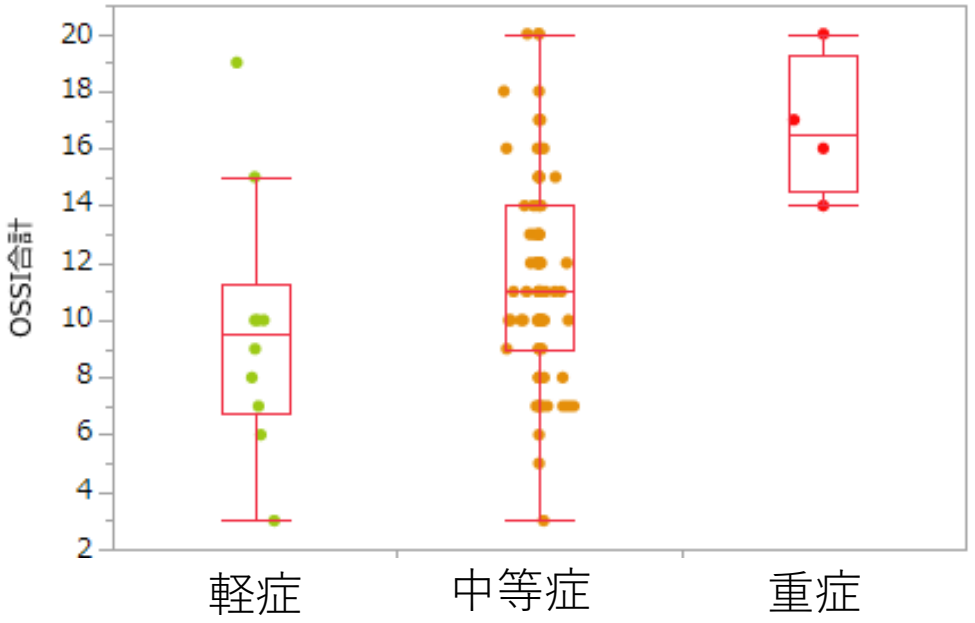

重症度分類とQOL

HIC (n=290)

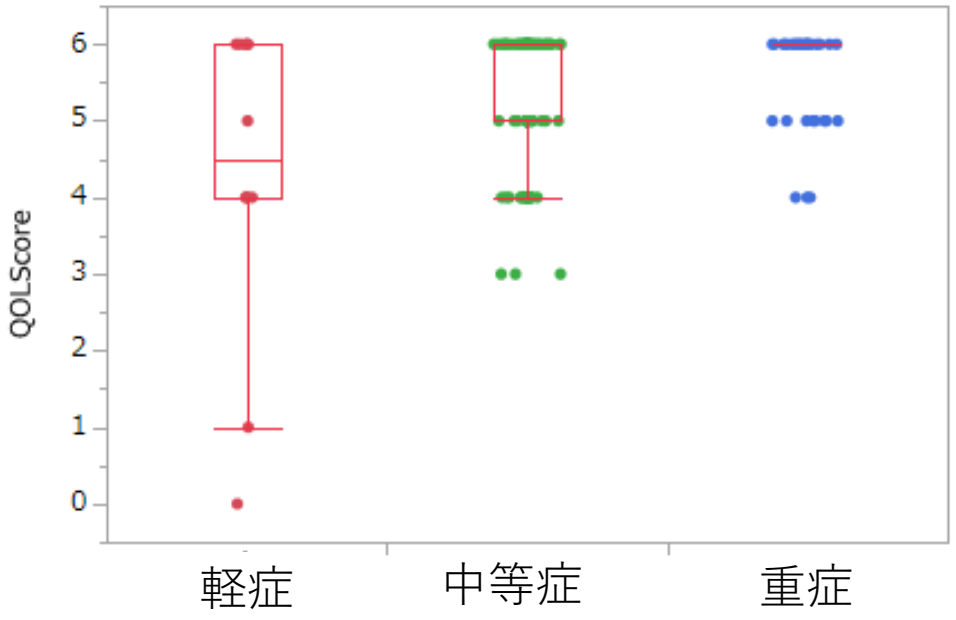

BPS (n=145)

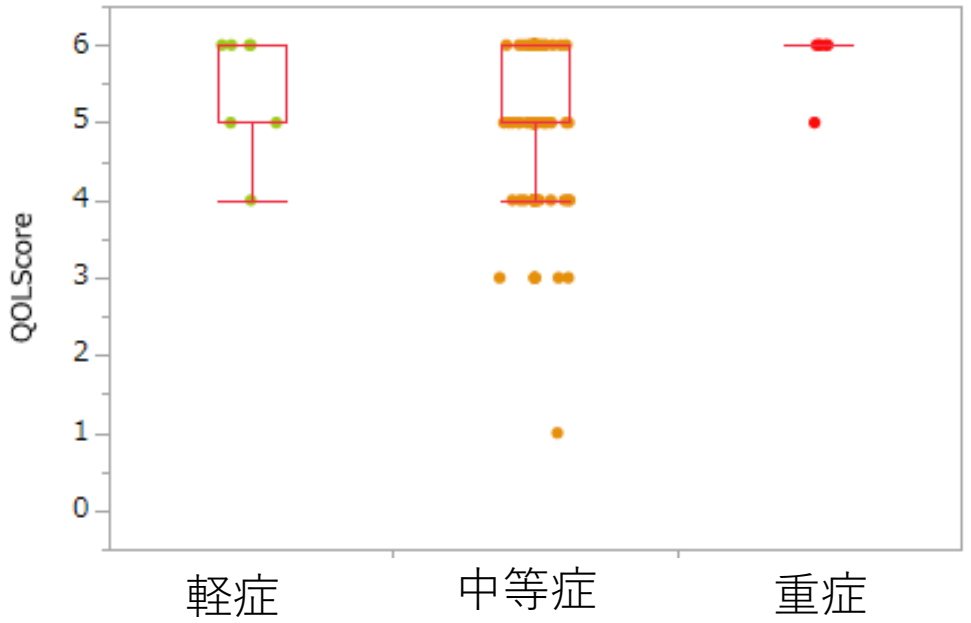

令和 3-5 年度 厚生労働科学研究費補助金

（難治性疾患政策研究事業）

「間質性膀胱炎の患者登録と診療ガイドラインに関する研究」

令 和 5 年 度 第 1 回　班会議　プ ロ グ ラ ム

2024 年 1 月 21 日（日）10：00～12：00

現地および WEB 開催

東京大学医学部泌尿器科学教室内

主任研究者　本間　之夫

10：00～10：05　　開会の挨拶、参加者の確認　　班長　本間之夫

10：05～10：10　　本研究班の目的と進捗状況の概要　　班長　本間之夫

10：10～11：00　　令和 5 年度事業成果報告　　東京大学　秋山佳之、新美文彩

休憩 10 分

11：10～11：50　　協議事項　　参加者全員

① 患者レジストリ
今後の見通し・方針
BPS の症例集積
他の難病に相当する疾患への応用
② 患者への情報提供・支援活動
冊子の配布
患者会の支援
③ 標準化
内視鏡 AI 診断
病理 AI 診断、スコア化
ガイドラインの改定？

11：50～12：00　　総括　　班長　本間之夫

available at www.sciencedirect.com
journal homepage: www.eu-openscience.europeanurology.com

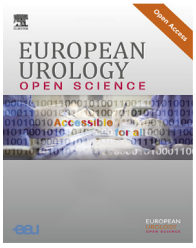

European Association of Urology

Pelvic Pain

Deep Learning Models for Cystoscopic Recognition of Hunner Lesion in Interstitial Cystitis

Takuya Iwaki[a,b,c], *Yoshiyuki Akiyama*[a,*], *Hirokazu Nosato*[c], *Manami Kinjo*[d], *Aya Niimi*[a,e], *Satoru Taguchi*[a], *Yuta Yamada*[a], *Yusuke Sato*[a], *Taketo Kawai*[f], *Daisuke Yamada*[a], *Hidenori Sakanashi*[c], *Haruki Kume*[a], *Yukio Homma*[g], *Hiroshi Fukuhara*[d]

[a] *Department of Urology, Graduate School of Medicine, The University of Tokyo, Tokyo, Japan;* [b] *Department of Urology, Center Hospital of the National Center for Global Health and Medicine, Tokyo, Japan;* [c] *Artificial Intelligence Research Center, National Institute of Advanced Industrial Science and Technology, Tsukuba, Japan;* [d] *Department of Urology, Kyorin University School of Medicine, Tokyo, Japan;* [e] *Department of Urology, New Tokyo Hospital, Matsudo, Japan;* [f] *Department of Urology, Teikyo University School of Medicine, Tokyo, Japan;* [g] *Japanese Red Cross Medical Center, Tokyo, Japan*

Article info

Article history:
Accepted December 22, 2022

Associate Editor:
Véronique Phé

Keywords:
Artificial intelligence
Interstitial cystitis
Bladder pain syndrome
Hunner lesion
Deep learning

Abstract

Background: Accurate cystoscopic recognition of Hunner lesions (HLs) is indispensable for better treatment prognosis in managing patients with Hunner-type interstitial cystitis (HIC), but frequently challenging due to its varying appearance.
Objective: To develop a deep learning (DL) system for cystoscopic recognition of a HL using artificial intelligence (AI).
Design, setting, and participants: A total of 626 cystoscopic images collected from January 8, 2019 to December 24, 2020, consisting of 360 images of HLs from 41 patients with HIC and 266 images of flat reddish mucosal lesions resembling HLs from 41 control patients including those with bladder cancer and other chronic cystitis, were used to create a dataset with an 8:2 ratio of training images and test images for transfer learning and external validation, respectively. AI-based five DL models were constructed, using a pretrained convolutional neural network model that was retrained to output 1 for a HL and 0 for control. A five-fold cross-validation method was applied for internal validation.
Outcome measurements and statistical analysis: True- and false-positive rates were plotted as a receiver operating curve when the threshold changed from 0 to 1. Accuracy, sensitivity, and specificity were evaluated at a threshold of 0.5. Diagnostic performance of the models was compared with that of urologists as a reader study.
Results and limitations: The mean area under the curve of the models reached 0.919, with mean sensitivity of 81.9% and specificity of 85.2% in the test dataset. In the reader study, the mean accuracy, sensitivity, and specificity were, respectively, 83.0%, 80.4%, and 85.6% for the models, and 62.4%, 79.6%, and 45.2% for expert urologists. Limitations include the diagnostic nature of a HL as warranted assertibility.

* Corresponding author. Department of Urology, Graduate School of Medicine, The University of Tokyo, 7-3-1 Hongo, Bunkyo, Tokyo 113-8655, Japan. Tel. +81 35 800 8753; Fax: +81 35 800 8917.
E-mail address: akiyamay-uro@h.u-tokyo.ac.jp (Y. Akiyama).

https://doi.org/10.1016/j.euros.2022.12.012

Conclusions: We constructed the first DL system that recognizes HLs with accuracy exceeding that of humans. This AI-driven system assists physicians with proper cystoscopic recognition of a HL.

Patient summary: In this diagnostic study, we developed a deep learning system for cystoscopic recognition of Hunner lesions in patients with interstitial cystitis. The mean area under the curve of the constructed system reached 0.919 with mean sensitivity of 81.9% and specificity of 85.2%, demonstrating diagnostic accuracy exceeding that of human expert urologists in detecting Hunner lesions. This deep learning system assists physicians with proper diagnosis of a Hunner lesion.

1. Introduction

Interstitial cystitis (IC) and bladder pain syndrome (BPS) represent a chronic debilitating disorder characterized by persistent pelvic pain associated with lower urinary tract symptoms [1]. IC/BPS can be divided into two subtypes based on cystoscopic findings: Hunner-type IC (HIC, having Hunner lesions), which corresponds to the International Society for the Study of IC/BPS (ESSIC) BPS type 3, and BPS (lackingHunner lesions), corresponding to ESSIC BPS types 1 and 2 [1–3]. Growing evidence has revealed that these two subtypes are different in terms of clinical characteristics, bladder pathology, and gene expression profiles, suggesting distinct causes of pathogenesis [4–8]. Hence, treatment strategies should be devised separately in a subtype-directed manner, and proper recognition of a Hunner lesion is of great importance [3]. However, there have been no objective and standardized diagnostic criteria for a Hunner lesion, and thus diagnosis of HIC is made subjectively by physicians based on cystoscopic findings and other clinical information including patient's characteristics and demographics. In addition, Hunner lesions vary in appearance, which can make recognition challenging [9] and may explain the variable frequency of the Hunner lesion subtype reported around the world [8].

Artificial intelligence (AI), especially deep learning, has increasingly been applied in medical fields, especially in diagnostic imaging [10–14]. Previous research has demonstrated that deep learning models can exceed the abilities of humans to detect several diseases, including bladder cancer [11,15–18]. Herein, we developed a computer-aided diagnosis (CAD) system for Hunner lesions by applying a pretrained convolutional neural network (CNN), the most frequently used and established deep learning algorithm for image-data classification, which distinguished Hunner lesions from other confusable flat reddish mucosal lesions with higher accuracy than IC/BPS-proficient physicians.

2. Patients and methods

2.1. Ethics statement

This study was approved by the Institutional Review Board of the University of Tokyo Hospital (no. 2019114NI), Kyorin University Hospital (no. H30-182), and National Institute of Advanced Industrial Science and Technology (no. Hi2019-304). All participants were informed about this study using generally accessible contact information, and written informed consent was obtained from patients who chose to participate. All procedures followed appropriate guidelines.

2.2. Participants and cystoscopic image preparation

A total of 82 participants were enrolled in this study, including 41 patients with HIC who had undergone and responded to endoscopic surgery (electrocautery of Hunner lesions with bladder hydrodistension), and 41 control patients who had flat reddish mucosal lesions in their bladders and underwent transurethral resection/biopsy of the lesions at the University of Tokyo Hospital from January 8, 2019 to December 24, 2020. All surgeries were performed under general or spinal anesthesia on an inpatient basis. The flat reddish mucosal lesions were carefully searched and cystoscopically visualized, with the bladder minimally filled with normal saline. Diagnosis of HIC was made by two urologists with expertise in managing IC/BPS, both board members of the East Asian IC/BPS Clinical Guidelines Committee (Y.A. and Y.H.) [1], according to the East Asian clinical guidelines for IC/BPS, the American Urological Association guidelines for IC/BPS, and the ESSIC criteria [1,2,19,20].

Demographics of patients with HIC retrieved from medical records included the following: O'Leary and Sant's Symptom Index and Problem Index; an 11-point numerical rating of pain intensity, with 0 indicating no pain and 10 indicating maximum pain; a 7-grade quality of life scale derived from the International Prostate Symptom Score, with 0 indicating excellent and 6 indicating terrible; daytime and nocturnal urinary frequency; average and maximum voided volume; and bladder capacity measured during bladder hydrodistension at a pressure of 80 cmH_2O under general/spinal anesthesia. Paired cold cup biopsies of the Hunner lesion and nonlesion background mucosa were obtained and sent to the Department of Pathology for histological analysis. Diagnoses of control patients were made based on histology at surgery: 23 patients were diagnosed with non–muscle-invasive bladder cancer, including 20 with carcinoma in situ (CIS) and three with papillary urothelial carcinoma (pTa; one with high grade and two with low grade); eight patients exhibited histological evidence of subepithelial chronic inflammatory changes accompanied by granulomas, epithelial denudation and reactive atypia, and stromal edema in bladders that had undergone intravesical mycobacteria bacillus Calmette-Guérin (BCG) injection for previous bladder cancers, and were diagnosed with BCG-related cystitis; and ten patients were diagnosed with chronic cystitis unrelated to HIC or BCG, including one with malakoplakia and three with radiation cystitis having a previous history of radiation therapy for prostate cancer (two) or cervical cancer (one) [21]. Of the 20 patients with CIS, two had previously undergone intravesical BCG therapy. All control patients underwent transurethral resection/biopsy of the bladder tumors and/or the flat reddish mucosal lesions if suspected of bladder cancer, suggested by urine cytology class III or worse, and/or associated with asymp-

tomatic macrohematuria. All surgeries were performed using white-light rigid endoscopes (Olympus Medical System, Tokyo, Japan, or Karl Storz, Tuttlingen, Germany). Still cystoscopic images were obtained from the operative video records of each surgery. The flat reddish mucosal lesions resembling Hunner lesions in control patients served as control images for Hunner lesions, regardless of the presence or absence of malignancy.

2.3. A CAD model for Hunner lesions

We first processed cystoscopic images to highlight and correct differences between images obtained from the Olympus and Karl Storz cystoscopes. In each image, a region of interest (ROI) was outlined by a circle, and the color tone and brightness of the bladder mucosa within the ROI were corrected according to the color balance of that area. In addition, the area outside the ROI was replaced by snow noise that was adjusted to the corrected color tone of the ROI (Supplementary Fig. 1). Then, the processed cystoscopic images were randomly assigned to the training set (80%) for transfer learning of a CNN model and the test set (20%) for external validation.

We used InceptionResNetv2, a pretrained CNN model with >1 million natural images from the ImageNet database (http://www.image-net.org), for constructing our CAD models based on transfer learning, to compensate for the relatively small volume of training images (Supplementary Fig. 2) [22]. We employed a five-fold cross-validation method to evaluate our CAD models. Briefly, the training dataset was further randomly divided into five stratified subsets of equal size and proportion of Hunner lesion images. Among the five subsets, images from four subsets (ie, 80% of the training data) were used to retrain the pretrained CNN model, and images from the remaining subset (20% of the training data) were used to validate the retrained CNN models. In this process, the network parameters of the pretrained CNN model were transferred to the initial network parameters to learn the cystoscopic images according to the proposed method. Then, all network parameters were retrained using images of the four subsets in a supervised manner based on the Stochastic Gradient Descent algorithm to discern Hunner and control lesions and validated using images from the remaining subset to prevent overfitting in this CAD model. These steps were repeated five times by alternating each subset used as test images, yielding five CAD models. Subsequently, the performance of the constructed five CAD models was evaluated using the test dataset for external validation (Supplementary Fig. 2).

2.4. Reader study of diagnostic performance to compare CAD models with urologists

Next, we assessed the potential clinical utility of the constructed CAD models by comparing their diagnostic performance with that of urologists in a reader study. A 100-image dataset was created by randomly selecting 50 images each of Hunner lesions and control lesions from the test dataset (Supplementary Fig. 2). Five IC/BPS experts (defined as those who had performed ≥100 endoscopic surgeries for patients with HIC), 11 Japanese Urological Association board–certified urologists (those who had ≥6 yr of experience in urology), and eight urology residents (≤5 yr of experience in urology) classified each image of the selected 100-image dataset in a blinded manner.

2.5. Statistical analysis

The performance of the CAD models for Hunner lesions was evaluated by creating a receiver operating characteristic (ROC) curve. The CNN was retrained to output 1 if the image was of a Hunner lesion and 0 if of a control lesion. True- and false-positive rates were plotted on the ROC curve when the threshold changed from 0 to 1. The area under the curve (AUC) was calculated from the ROC curve. Accuracy, sensitivity, and specificity were evaluated at a threshold of 0.5.

3. Results

3.1. Participants and cystoscopic image preparation

The demographics of the patients are shown in Table 1. All patients with HIC favorably responded to electrocautery of Hunner lesions and manifested the histological characteristics of HIC, such as lymphoplasmacytic infiltration, epithelial denudation, stromal fibrosis, and edema in bladder pathology [4,5,20]. All control patients did not have lower urinary tract symptoms and/or chronic pelvic pain that needed treatments to be resolved.

A total of 626 images of 233 lesions in 82 surgeries, including 360 images of 129 Hunner lesions and 266 images of 104 control lesions, were obtained (Table 2 and Fig. 1). A total of 338 images, including 236 images of Hunner lesions and 102 images of control lesions, were obtained using the Olympus rigid endoscope, and 288 images, including 124 images of Hunner lesions and 164 images of control lesions, were obtained using the Karl Storz rigid endoscope. Of the 266 control images, 136 were of CIS, 14 of urothelial carcinoma, 78 of BCG cystitis, 11 of radiation cystitis, two of malakoplakia, and 25 of other chronic cystitis (Supplementary Table 1). The training dataset contained 500 images, including 288 of Hunner lesions and 212 of control lesions, and the test dataset contained 126 images, including 72 of Hunner lesions and 54 of control lesions.

3.2. Diagnostic performance of the constructed models

The mean AUC of the five constructed CAD models was 0.919 in the test image dataset for external validation, with mean sensitivity of 81.9% and specificity of 85.2% at a threshold of 0.5 (Fig. 2A). In a reader study, the mean accuracy, sensitiv-

Table 1 – Demographics of study participants

	HIC	Control
No. (male/female)	41 (5/36)	41 (30/11)
Mean age at surgery (yr)	67.6 ± 11.8 (42–83) [a]	74.6 ± 9.2 (45–94)
Years from symptom onset to surgery	3.8 ± 3.7 (1–18)	NA
OSSI	14.9 ± 4.6 (5–20)	NA
OSPI	12.7 ± 3.7 (3–16)	NA
Pain intensity [b]	7.7 ± 1.8 (4–10)	NA
QOL score [c]	5.6 ± 0.9 (2–6)	NA
Daytime frequency	13.5 ± 5.7 (5–30)	NA
Nocturia frequency	4.7 ± 2.6 (0–12)	NA
Average voided volume (ml)	101.5 ± 47.8 (30–227)	NA
Maximum voided volume (ml)	164.6 ± 80.6 (50–350)	NA
Maximum bladder capacity at hydrodistension (ml)	426.9 ± 181.0 (150–1000)	NA

HIC = Hunner-type interstitial cystitis; NA = not analyzed; OSPI = O'Leary and Sant's Problem Index; OSSI = O'Leary and Sant's Symptom Index; QOL = quality of life; SD =standard deviation.

[a] Mean ± SD (range).

[b] Assessed using an 11-point pain intensity numerical rating scale ranging from 0, indicating no pain, to 10, indicating maximum pain.

[c] Assessed on a 7-grade QOL scale derived from the International Prostate Symptom Score, with 0 indicating excellent and 6 indicating terrible.

Table 2 – Demographics of cystoscopic image data

	HIC	Control		
		UC [a]	BCG [b]	Chronic cystitis [c]
No. of surgeries	41	41		
		23	8	10
No. of images (Olympus)	360 (236)	266 (102)		
		150 (47)	78 (30)	38 (25)
No. of lesions	129	104		
		57	26	21
Mean number of images per lesion	2.8	2.53		
		2.6	3	1.8

BCG = bacillus Calmette-Guérin; HIC = Hunner-type interstitial cystitis; UC = urothelial carcinoma.
[a] Urothelial carcinoma, including carcinoma in situ (20) and papillary urothelial carcinoma (three).
[b] Bacillus Calmette-Guérin–related cystitis.
[c] Chronic cystitis unrelated to BCG cystitis, including radiation cystitis (three) and malakoplakia (one).

ity, and specificity (at a threshold of 0.5) were, respectively, 83.0%, 80.4%, and 85.6% for the five models; 62.4%, 79.6%, and 45.2% for the IC/BPS expert physicians; 51.0%, 40.0%, and 62.0% for the Japanese Urological Association board–certified urologists; and 46.8%, 36.0%, and 57.8% for the urology residents. The diagnostic accuracy of the five models for Hunner lesions (mean AUC of 0.912) exceeded that of the IC/BPS expert physicians (Fig. 2B). Prediction of each image by the CAD models and humans was depicted as a heatmap and box plot (Supplementary Fig. 3 and 4). The results suggested that humans are likely to misrecognize control lesions for Hunner lesions, rather than vice versa.

3.3. *Heatmap visualization*

Examples of Hunner and control lesions correctly recognized by the CAD models are shown as heatmap visualization in Figure 3, in which areas that were important for diagnosis processing are highlighted. The CAD models seemed to preferentially assess the region of a reddened mucosal area accompanied by radiating/surrounding small vessels in the vicinity for differentiation between images of Hunner and control lesions. Images of control lesions that

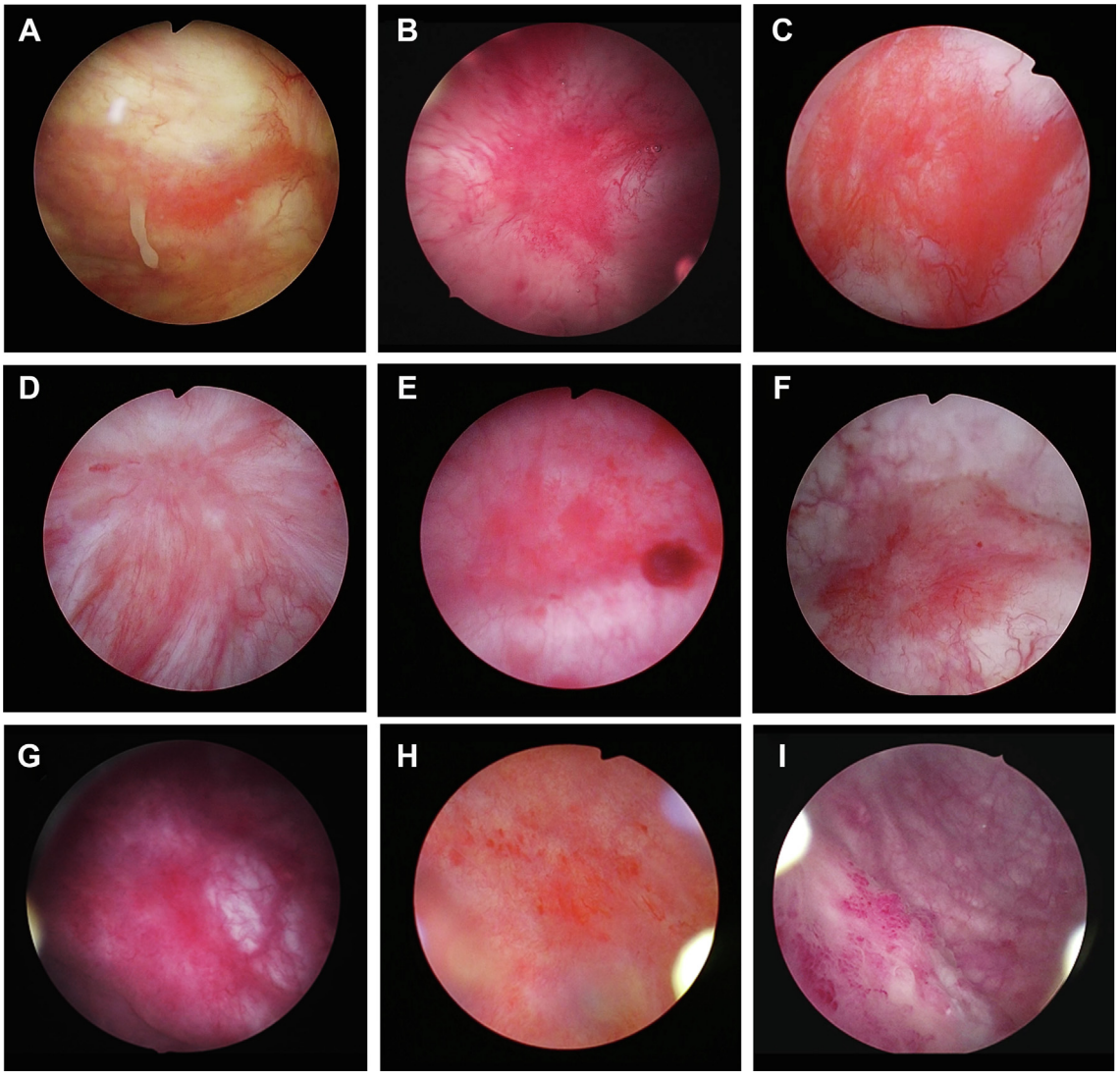

Fig. 1 – Representative cystoscopic images of Hunner lesions and control lesions. Representative images of preprocessed cystoscopic images including (A–C) Hunner lesions, (D and E) BCG cystitis, (F) radiation cystitis, (G) chronic cystitis, (H) CIS, and (I) UC. BCG = bacillus Calmette-Guérin; CIS = carcinoma in situ; UC = urothelial carcinoma.

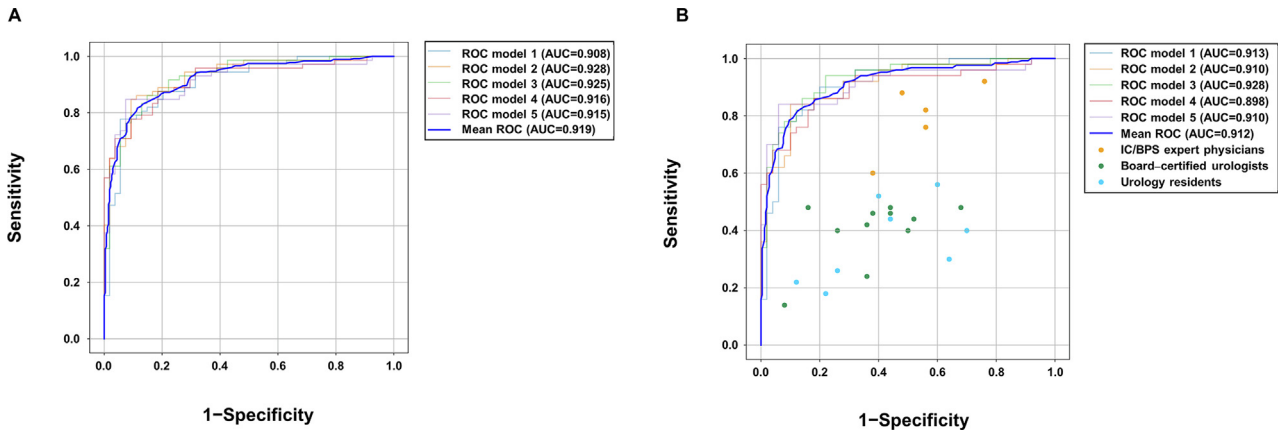

Fig. 2 – ROC curves for the five constructed deep learning models. (A) ROC curves for the five constructed deep learning models using the test dataset. (B) ROC curves for the five constructed deep learning models and the operating points of human urologists in the reader study. AUC = area under the curve; BPS = bladder pain syndrome; IC = Interstitial cystitis; ROC = receiver operating characteristic.

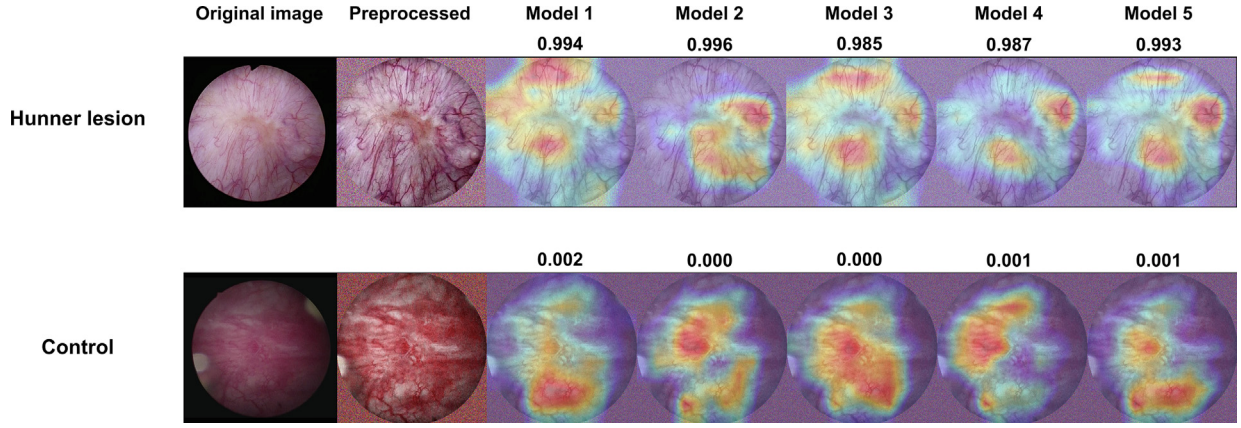

Fig. 3 – Heatmap visualization of Hunner and control images correctly recognized by the deep learning models. The heatmaps, created using Gradient-weighted Class Activation Mapping software, highlight the important regions in cystoscopic images for correctly predicting Hunner and control lesions. Vessels that cluster radially toward or surround the lesions were highlighted. These features might be responsible for image recognition by the deep learning models. The upper number of each heatmap image indicates the value predicted by the models (0, control, and 1, Hunner lesion).

all IC/BPS expert physicians unanimously misrecognized as Hunner lesions but all five CAD models correctly predicted as control lesions are shown in Supplementary Figure 5. The CAD models seemed to discriminate the images by focusing on features including specific capillary structures that IC/BPS expert physicians were not likely to fully notice during cystoscopy.

4. Discussion

In the present study, we developed an AI-driven CAD system for supporting cystoscopic recognition of a Hunner lesion based on a deep learning algorithm. The constructed models achieved a mean AUC of 0.912, sensitivity of 80.4%, and specificity of 85.6% for the detection of Hunner lesions, which outperformed the diagnostic accuracy of IC/BPS expert physicians.

A Hunner lesion, a characteristic reddish mucosal lesion frequently accompanied by abnormal capillary structures, is a hallmark of HIC. Although the etiology of a Hunner lesion remains elusive, it has been suggested that locally intensified inflammatory responses, in conjunction with ischemia, may be associated with the pathogenesis of a Hunner lesion [23]. This characteristic bladder lesion has crucial implications for diagnosis and treatment prognosis in HIC. In clinical management, Hunner lesion–targeted therapies such as local electrocautery or steroid injection provide more favorable outcomes than other treatment options in patients with HIC [24,25]. However, there have been no objective diagnostic markers for cystoscopic recognition of a Hunner lesion, and its appearance is highly variable [9]. Such lack of objectivity and variability in cystoscopic appearance, in addition to the extremely low prevalence of the Hunner lesion subtype, make recognition of a Hunner lesion challenging for the majority of urologists who do not have as much expertise as expert physicians in managing IC/BPS.

AI and deep learning techniques have successfully been applied in medical image diagnosis. Examples include dermoscopic diagnosis of melanoma [11,15], detection of

diabetic retinopathy in retinal fundus photographs [26], endoscopic diagnosis and progression assessment of gastric cancer [13], classification and mutation prediction of lung cancer using histological images [14], and prediction of genomic features and the response to immune checkpoint therapies of various cancers from histological images [27]. In urology, Shkolyar et al [16] developed deep learning models that detected bladder cancer with sensitivity of 90.9% and specificity of 98.6%. Ali et al [17] developed an AI diagnostic platform using blue-light cystoscopic images that not only detected bladder cancer with high sensitivity of 95.77% and modest specificity of 87.84%, but also classified tumor invasiveness with sensitivity of 88% and specificity of 96.56%. Tokuyama et al [28] developed AI models that predicted early recurrence of non–muscle-invasive bladder cancer with a probability of up to 90% based on machine learning of nuclear features in histological images. Yamamoto et al [12] developed a deep learning algorithm based on the assessment of histological images that accurately predicted recurrence of prostate cancer. These studies consistently demonstrated that deep learning models exert higher diagnostic ability in conjunction with human performance than when using either method alone. Collectively, AI and deep learning techniques have the potential to surpass limitations on conventional image diagnosis performed by humans only.

There are several limitations to this study that relate to the methodology, first among which is the opaque black box nature of AI-based deep learning techniques. Second, this study was performed using images that were acquired only by rigid cystoscopes. The appearance of cystoscopic images may vary depending on the light source and type of cystoscope. The versatility of our CAD models is to be validated using images obtained by other types of light sources or cystoscopes, including flexible cystoscopes. Third, the retrospective study design and the diagnostic nature of a Hunner lesion as warranted assertibility might bias cystoscopic image collection and thereby affect the results. Diagnosis of a Hunner lesion was made by our two urologists in a subjective manner, and thereby it might act as a working hypothesis in the present study. With regard to this, we used images of Hunner lesions that were obtained from cases that favorably responded to electrocautery of the lesions and showed characteristic histological features consistent with HIC [4,5,20]. Conversely, this might exclude some HIC cases that did not show those clinical and histological features, and could be another limitation of the present study. Objective, reliable, and reproducible diagnostic markers for a Hunner lesion are urgently needed to standardize the diagnosis of a Hunner lesion. Further multicenter, international prospective studies are warranted to verify the clinical utility of our CAD models in real-world settings.

5. Conclusions

We first developed the deep learning system that recognizes Hunner lesions in cystoscopic images with accuracy (mean AUC up to 0.912) greater than that of IC/BPS expert physicians. Our models provide a platform for developing a system that supports the accurate diagnosis of a Hunner lesion and that can lead to improved treatment outcomes in managing patients with HIC.

Author contributions: Yoshiyuki Akiyama had full access to all the data in the study and takes responsibility for the integrity of the data and the accuracy of the data analysis.

Study concept and design: Iwaki, Akiyama, Nosato, Fukuhara.
Acquisition of data: Iwaki, Akiyama.
Analysis and interpretation of data: Iwaki, Nosato.
Drafting of the manuscript: Iwaki, Akiyama, Nosato, Homma.
Critical revision of the manuscript for important intellectual content: Nosato, Kinjo, Niimi, Taguchi, Y. Yamada, Sato, Kawai, D. Yamada, Sakanashi, Kume, Homma, Fukuhara.
Statistical analysis: Iwaki, Nosato.
Obtaining funding: Akiyama.
Administrative, technical, or material support: Akiyama, Nosato.
Supervision: Akiyama, Homma, Fukuhara.
Other: None.

Financial disclosures: Yoshiyuki Akiyama certifies that all conflicts of interest, including specific financial interests and relationships and affiliations relevant to the subject matter or materials discussed in the manuscript (eg, employment/affiliation, grants or funding, consultancies, honoraria, stock ownership or options, expert testimony, royalties, or patents filed, received, or pending), are the following: None.

Funding/Support and role of the sponsor: This study was financially supported by a KAKENHI Grants-in-Aid from the Japanese Society for the Promotion of Science (JSPS; grant number 22K16788, to Yoshiyuki Akiyama).

Acknowledgments: This paper is partly based on the results obtained from a project, JPNP20006, commissioned by New Energy and Industrial Technology Development Organization (NEDO).

Appendix A. Supplementary data

Supplementary data to this article can be found online at https://doi.org/10.1016/j.euros.2022.12.012.

References

[1] Homma Y, Akiyama Y, Tomoe H, et al. Clinical guidelines for interstitial cystitis/bladder pain syndrome. Int J Urol 2020;27:578–89.
[2] van de Merwe JP, Nordling J, Bouchelouche P, et al. Diagnostic criteria, classification, and nomenclature for painful bladder syndrome/interstitial cystitis: an ESSIC proposal. Eur Urol 2008;53:60–7.
[3] Akiyama Y, Hanno P. Phenotyping of interstitial cystitis/bladder pain syndrome. Int J Urol 2019;26:17–9.
[4] Johansson SL, Fall M. Clinical features and spectrum of light microscopic changes in interstitial cystitis. J Urol 1990;143:1118–24.
[5] Maeda D, Akiyama Y, Morikawa T, et al. Hunner-type (classic) interstitial cystitis: a distinct inflammatory disorder characterized by pancystitis, with frequent expansion of clonal B-cells and epithelial denudation. PLoS One 2015;10:e0143316.
[6] Akiyama Y, Luo Y, Hanno PM, Maeda D, Homma Y. Interstitial cystitis/bladder pain syndrome: the evolving landscape, animal models and future perspectives. Int J Urol 2020;27:491–503.
[7] Watanabe D, Akiyama Y, Niimi A, et al. Clinical characterization of interstitial cystitis/bladder pain syndrome in women based on the presence or absence of Hunner lesions and glomerulations. Low Urin Tract Symptoms 2021;13:139–43.
[8] Fall M, Nordling J, Cervigni M, et al. Hunner lesion disease differs in diagnosis, treatment and outcome from bladder pain syndrome: an ESSIC working group report. Scand J Urol 2020;54:91–8.

[9] Ronstrom C, Lai HH. Presenting an atlas of Hunner lesions in interstitial cystitis which can be identified with office cystoscopy. Neurourol Urodyn 2020;39:2394–400.
[10] Shen Y, Shamout FE, Oliver JR, et al. Artificial intelligence system reduces false-positive findings in the interpretation of breast ultrasound exams. Nat Commun 2021;12:5645.
[11] Pham TC, Luong CM, Hoang VD, Doucet A. AI outperformed every dermatologist in dermoscopic melanoma diagnosis, using an optimized deep-CNN architecture with custom mini-batch logic and loss function. Sci Rep 2021;11:17485.
[12] Yamamoto Y, Tsuzuki T, Akatsuka J, et al. Automated acquisition of explainable knowledge from unannotated histopathology images. Nat Commun 2019;10:5642.
[13] Hirasawa T, Aoyama K, Tanimoto T, et al. Application of artificial intelligence using a convolutional neural network for detecting gastric cancer in endoscopic images. Gastric Cancer 2018;21:653–60.
[14] Coudray N, Ocampo PS, Sakellaropoulos T, et al. Classification and mutation prediction from non-small cell lung cancer histopathology images using deep learning. Nat Med 2018;24:1559–67.
[15] Haenssle HA, Fink C, Schneiderbauer R, et al. Man against machine: diagnostic performance of a deep learning convolutional neural network for dermoscopic melanoma recognition in comparison to 58 dermatologists. Ann Oncol 2018;29:1836–42.
[16] Shkolyar E, Jia X, Chang TC, et al. Augmented bladder tumor detection using deep learning. Eur Urol 2019;76:714–8.
[17] Ali N, Bolenz C, Todenhofer T, et al. Deep learning-based classification of blue light cystoscopy imaging during transurethral resection of bladder tumors. Sci Rep 2021;11:11629.
[18] Ikeda A, Nosato H, Kochi Y, et al. Support system of cystoscopic diagnosis for bladder cancer based on artificial intelligence. J Endourol 2020;34:352–8.
[19] Hanno PM, Burks DA, Clemens JQ, et al. AUA guideline for the diagnosis and treatment of interstitial cystitis/bladder pain syndrome. J Urol 2011;185:2162–70.
[20] Akiyama Y, Homma Y, Maeda D. Pathology and terminology of interstitial cystitis/bladder pain syndrome: a review. Histol Histopathol 2019;34:25–32.
[21] Lopez-Beltran A, Luque RJ, Mazzucchelli R, Scarpelli M, Montironi R. Changes produced in the urothelium by traditional and newer therapeutic procedures for bladder cancer. J Clin Pathol 2002;55:641–7.
[22] Szegedy C, Ioffe S, Vanhoucke V, Alemi AA. Inception-v4, Inception-ResNet and the impact of residual connections on learning. Thirty-first AAAI Conference on Artificial Intelligence; 2017.
[23] Akiyama Y, Miyakawa J, O'Donnell MA, et al. Overexpression of HIF1alpha in Hunner lesions of interstitial cystitis: pathophysiological implications. J Urol 2022;207:635–46.
[24] Hillelsohn JH, Rais-Bahrami S, Friedlander JI, et al. Fulguration for Hunner ulcers: long-term clinical outcomes. J Urol 2012;188: 2238–41.
[25] Funaro MG, King AN, Stern JNH, Moldwin RM, Bahlani S. Endoscopic injection of low dose triamcinolone: a simple, minimally invasive, and effective therapy for interstitial cystitis with Hunner lesions. Urology 2018;118:25–9.
[26] Gulshan V, Peng L, Coram M, et al. Development and validation of a deep learning algorithm for detection of diabetic retinopathy in retinal fundus photographs. JAMA 2016;316:2402–10.
[27] Komura D, Kawabe A, Fukuta K, et al. Universal encoding of pan-cancer histology by deep texture representations. Cell Rep 2022;38:110424.
[28] Tokuyama N, Saito A, Muraoka R, et al. Prediction of non-muscle invasive bladder cancer recurrence using machine learning of quantitative nuclear features. Mod Pathol 2022;35:533–8.

ハンナ型間質性膀胱炎の内視鏡診断支援システム

～Webサービスアプリの紹介～

2024年1月21日（日）

国立研究開発法人 産業技術総合研究所
人工知能研究センター 機械学習機構研究チーム
研究チーム長　野里博和

間質性膀胱炎（ハンナ型）病理組織グレーディング構築

Epithelial damage grade		
Epithelial denudation	None or subtle	0
	Mild	1
	Moderate	2
	Severe	3
Sloughing pattern of denudation	Absent	0
	Present	1
Fibrinous exudate (erosive change)	Absent	0
	Present	1
Intraepithelial lymphocytes	None	0
	Scattered	1
	Dense	2

Stromal inflammation grade		
Subepithelial lymphoplasmacytic infiltration	None or subtle	0
	Mild	1
	Moderate	2
	Severe	3
Lymphocytic aggregate/Lymphoid follicle	Absent	0
	Present	1
Plasma cell-rich area (more than 30%)	Absent	0
	Present	1
Marked eosinophilic infiltration (>50/HPF)	Absent	0
	Present	1
Marked neutrophilic infiltration (>50/HPF)	Absent	0
	Present	1

Fibrovascular alteration grade		
Prominent stromal fibrosis	Absent	0
	Present	1
Prominent vascular proliferation	Absent	0
	Present	1

これらの項目を評価した上で、HIC重症度との相関を解析し、nomogramを作成する方針

間質性膀胱炎（ハンナ型）
ゲノム研究成果報告

ハンナ型間質性膀胱炎の遺伝的背景を解明: HLA遺伝子領域に複数の疾患感受性遺伝子を同定

全ゲノム関連解析: GWAS

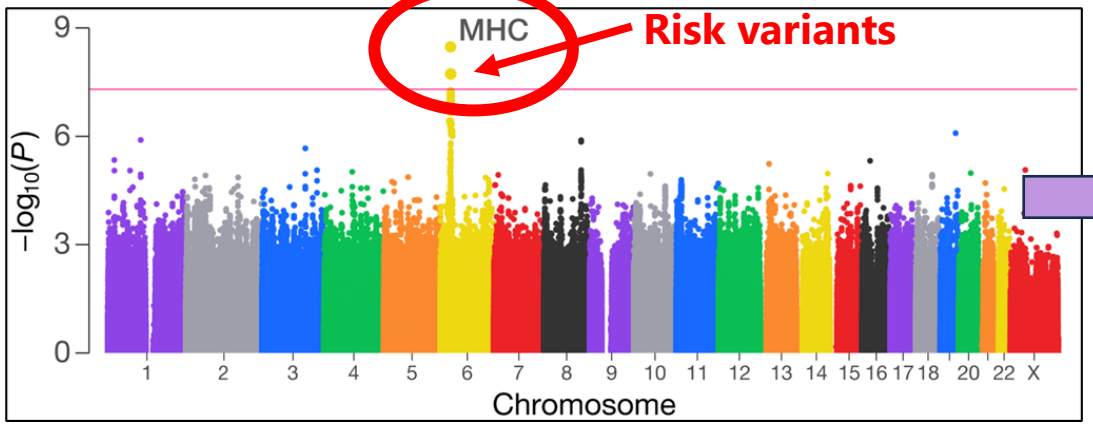

Fine-mapping analysis of HLA variants

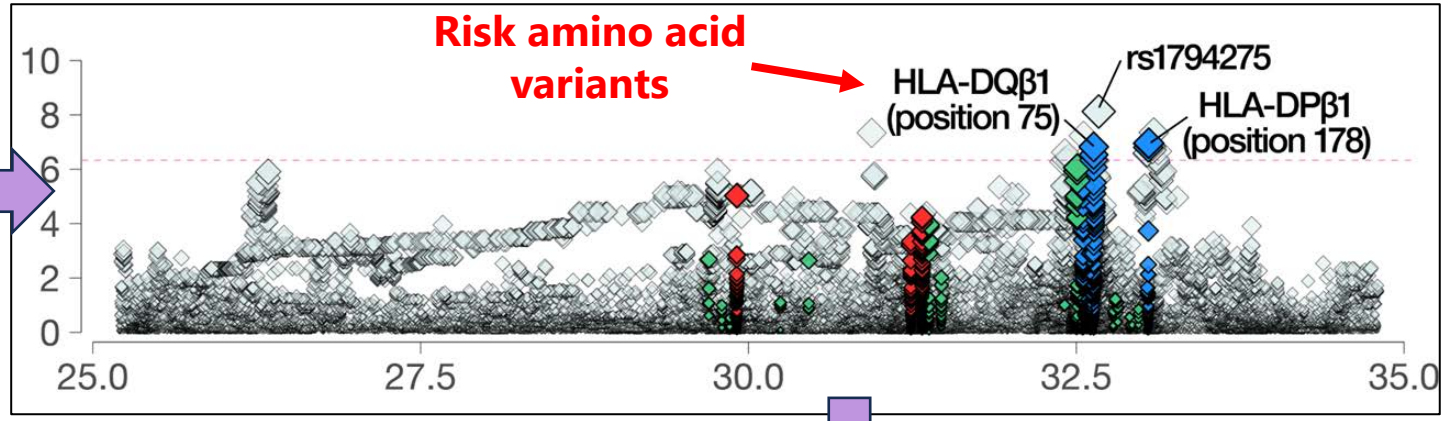

免疫異常を惹起

リスクバリアント保因者

抗原提示能の変化

B細胞系優位の免疫疾患を発症

間質性膀胱炎の本態に迫る成果

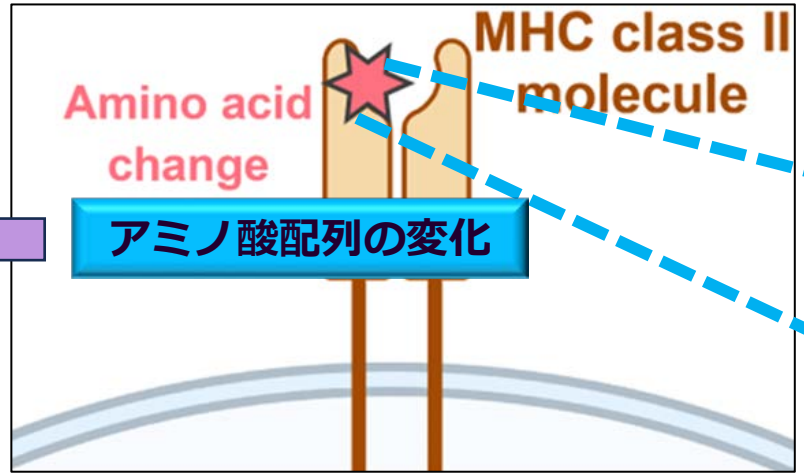

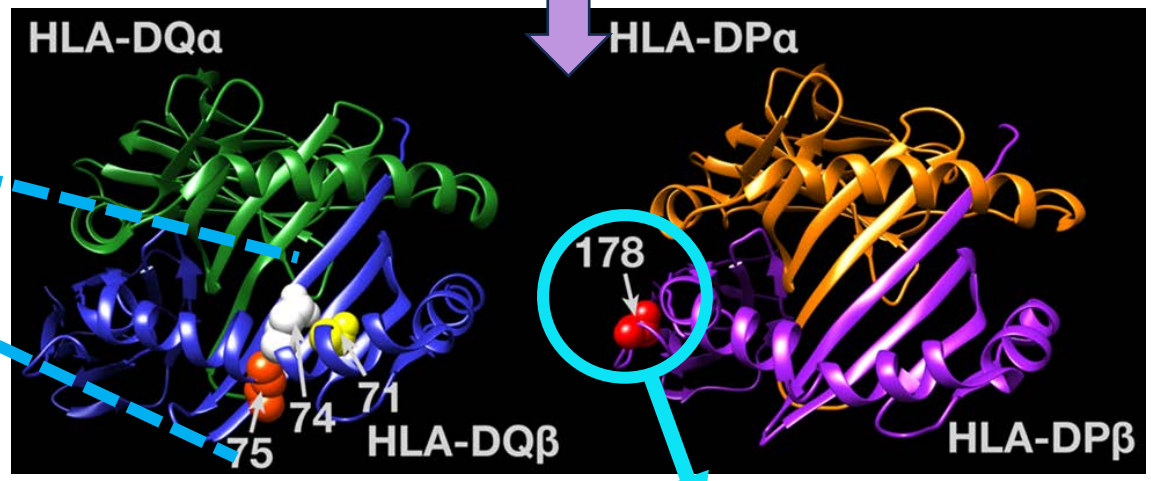

MHCクラスⅡ分子の抗原結合部位に存在し抗原提示能に関与

他の自己免疫疾患のリスクバリアント

間質性膀胱炎（ハンナ型）のGWAS：厚労科研オールジャパン体制で拡大実施中！

研究参加施設

- 旭川医科大学
- 北海道大学
- 札幌中央病院（札幌医大）
- 新東京病院
- 杏林大学
- 東京大学
- 関東労災病院
- 浜松医科大学
- 奈良県立医科大学
- 県立広島病院
- 原三信病院
- 長崎大学

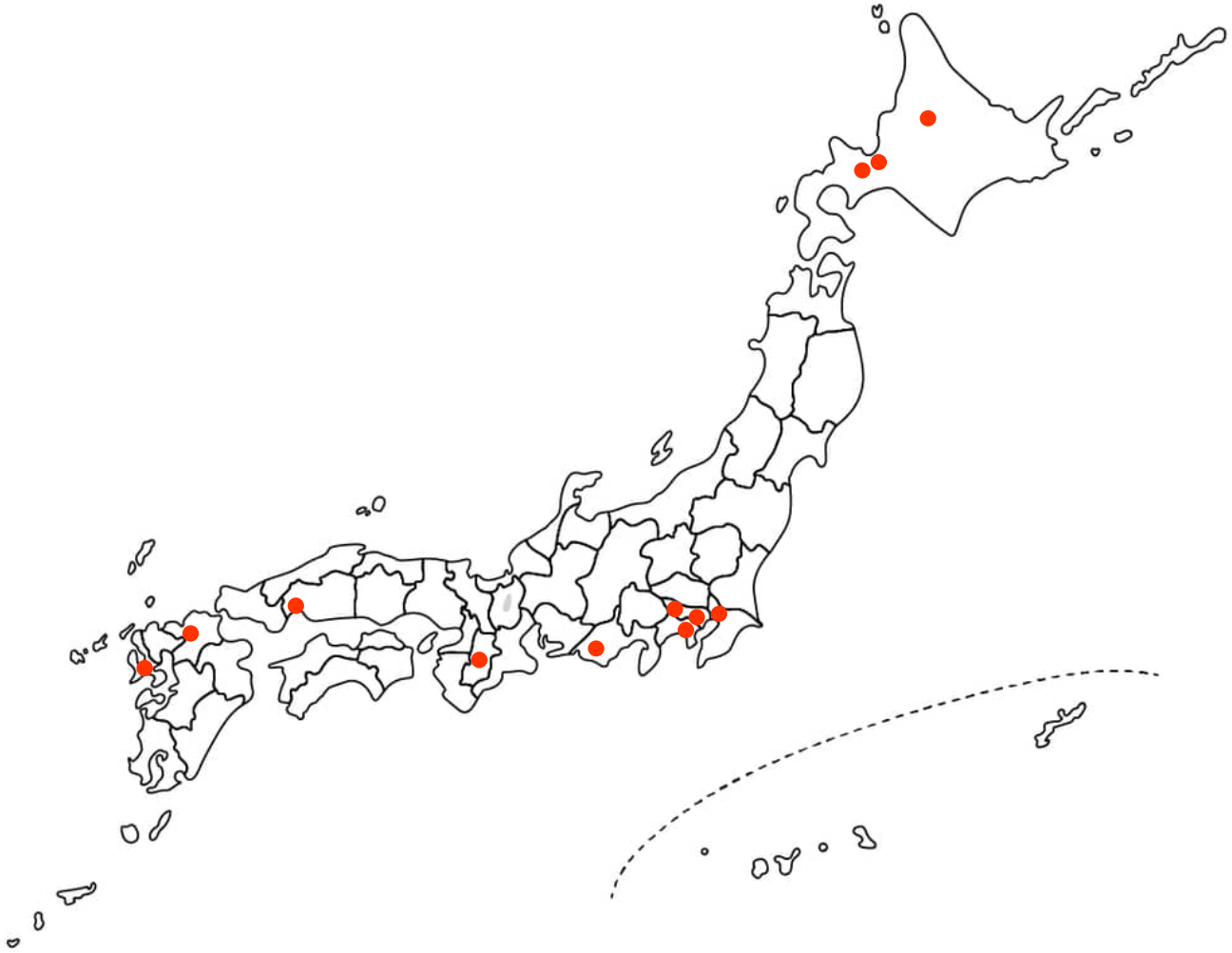

新規治療開発に関する研究

ハンナ型間質性膀胱炎の創薬ターゲットとしてIFN-γを特定

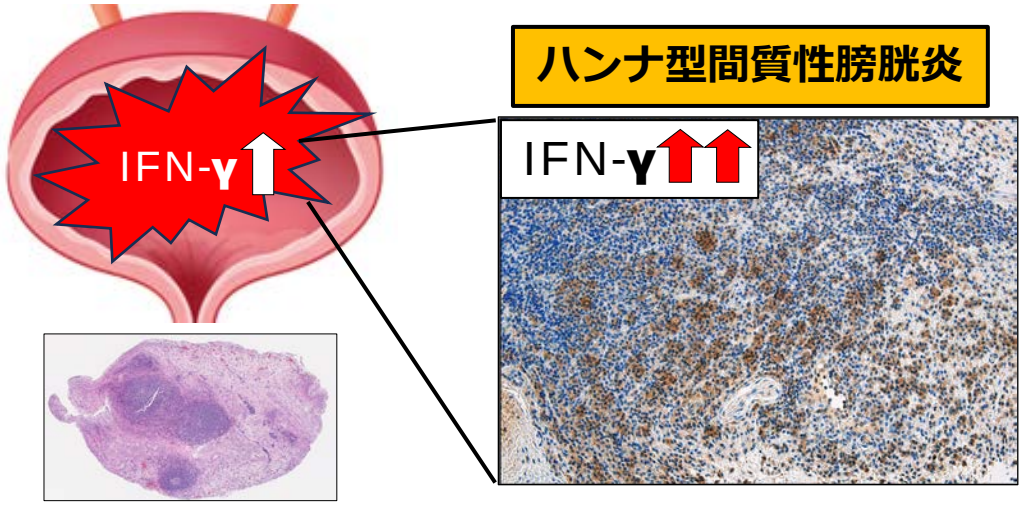

養子移植免疫による間質性膀胱炎モデル動物を開発

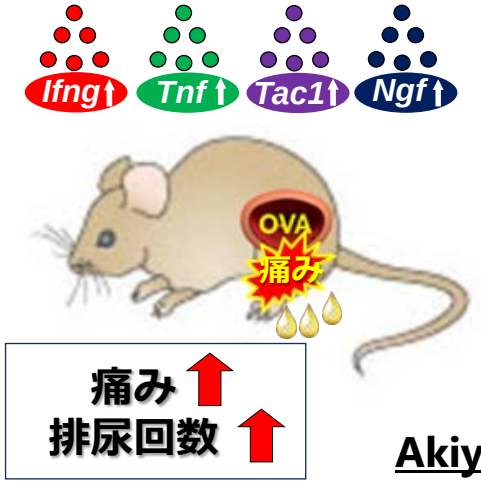

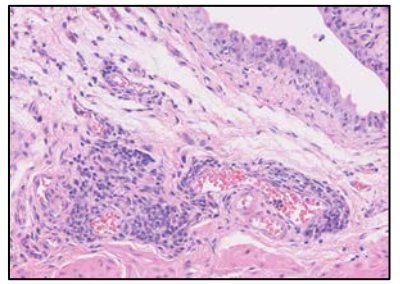

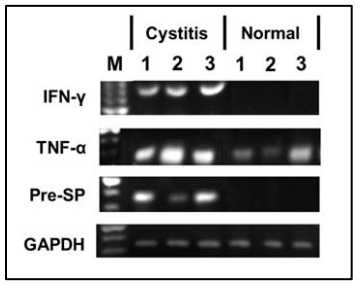

Akiyama Y et al. *Am J Physiol Renal Physiol*. 2021

核酸医薬によるanti-IFN-γ 膀胱内治療の開発

抗IFN-γ
DNA アプタマー

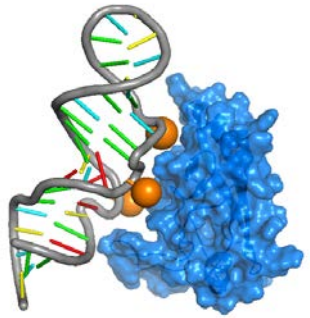

開発

間質性膀胱炎（ハンナ型）
疾患モデル

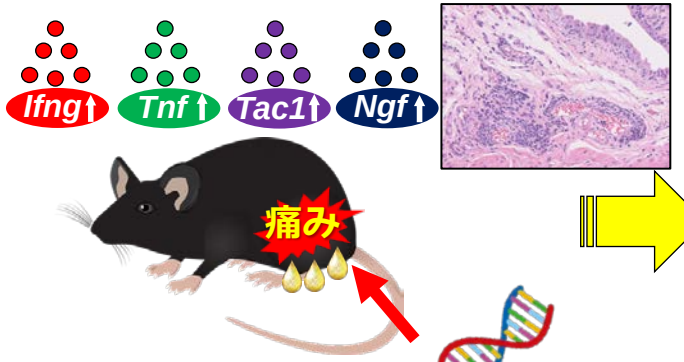

アプタマー
膀胱内投与

炎症反応/症状の大幅な改善

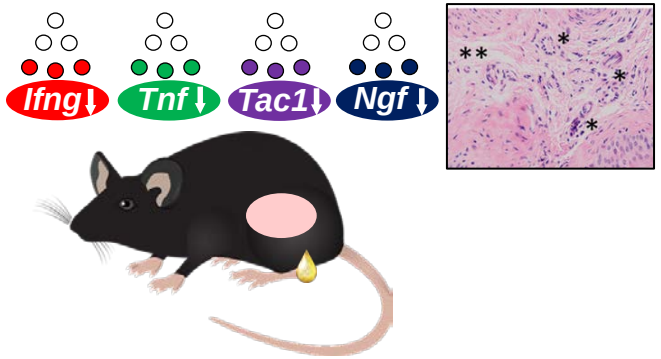

痛み
排尿回数

- POC確認完了
- GLP毒性・安全性薬理試験

ヒトへの臨床応用
新規治療法の開発へ

間質性膀胱炎の患者登録と診療ガイドラインに関する研究班

我々は平成２８年度に厚生労働省の難治性疾患政策研究事業の間質性膀胱炎研究班として発足し、以降、間質性膀胱炎に対する一般社会に対する啓発や難病支援体制の充実を目指して活動しています。

News

2024/04/30　第８回 研究班班会議を開催いたしました。（現地及びWeb）

2023/01/22　第７回 研究班班会議を開催しました。（Web開催）

2022/01/23　第６回 研究班班会議を開催しました。（Web開催）

TOP

患者さんの理解のために

間質性膀胱炎・膀胱痛症候群

著者
秋山佳之
新美文彩
野宮　明
本間之夫

医学図書出版

[目次]

著者：秋山　佳之，新美　文彩，野宮　　明，本間　之夫

ISBNコード：978-4-86517-510-3

発行年月日：2022年12月20日

サイズ・頁数：B5判・250頁